Available online at www.sciencedirect.com

ScienceDirect

journal homepage: www.elsevier.com/locate/he

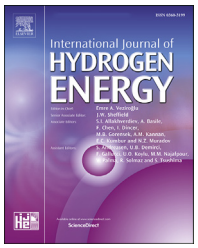

Review Article

Challenges associated with hydrogen storage systems due to the hydrogen embrittlement of high strength steels

Ujwal Shreenag Meda [a,b,*], *Nidhi Bhat* [a,b,**], *Aditi Pandey* [a,b], *K.N. Subramanya* [c], *M.A. Lourdu Antony Raj* [d]

[a] *Department of Chemical Engineering, RV College of Engineering, Bengaluru, India*
[b] *Centre for Hydrogen and Green Technology, RV College of Engineering, Bengaluru, India*
[c] *Department of Industrial Engineering and Management, RV College of Engineering, Bengaluru, India*
[d] *Department of Chemical Engineering, MVJ College of Engineering, Bengaluru, India*

HIGHLIGHTS

- High strength steels are avoided in hydrogen storage systems due to embrittlement.
- Assessing material's susceptibility to hydrogen permeation and trapping is crucial.
- Trace amounts of hydrogen penetrating the steel accumulates at the crack tips.
- Exposure time, material's microstructure and residual stresses are critical.
- Multi-layered coatings could significantly increase resistance to embrittlement.

ARTICLE INFO

Article history:
Received 6 December 2021
Received in revised form
2 January 2023
Accepted 24 January 2023
Available online 12 February 2023

ABSTRACT

Hydrogen is a promising alternative to fossil fuels and is extensively used in process industries. The transportation industry is gearing up towards the use of fuel cells where hydrogen, as a fuel, plays a major role. Irrespective of the application/sector, safe handling and storage of hydrogen are crucial. Storing hydrogen in metal cylinders as compressed gas is a common practice. However, hydrogen embrittlement is a challenge in such cases and needs to be addressed. Embrittlement leads to the deterioration of the metal cylinders in which the hydrogen gas is stored and is therefore a safety concern. High-strength steels are more susceptible to hydrogen embrittlement as susceptibility to the phenomenon increases with strength. Safe hydrogen storage systems demand improved storage materials and modification of existing ones. Few materials and methods are available to reduce hydrogen diffusion in these steels. However, a detailed microstructural analysis of high-strength steel is necessary to make it a hydrogen-impermeable material. Multilayered coatings can be effective in the prevention of embrittlement. In this article, the analysis of current hydrogen storage methods along with the various

* *Corresponding author*. Department of Chemical Engineering, RV College of Engineering, Bengaluru, India.
** *Corresponding author*.
E-mail addresses: ujwalshreenagm@rvce.edu.in (U.S. Meda), nidhibhat.ch19@rvce.edu.in (N. Bhat).
https://doi.org/10.1016/j.ijhydene.2023.01.292

coatings and deposition techniques that can reduce hydrogen permeation in high-strength steels is carried out.

Contents

Introduction

The ongoing exploitation of finite energy resources has shifted attention towards the world's future energy scenario in the face of fossil fuel shortage [1]. Numerous environmental challenges (acid rain, depletion of the ozone layer, climate change, global warming, etc.) have taken shape and are related to the production, transformation, and use of energy. Additionally, numerous industrial giants are attempting to lessen their reliance on fossil fuels [2]. To address the tremendous challenge of climate change, energy systems are undergoing a shift to technologies that reduce the emission of greenhouse gases (GHGs) [3].

Several potential remedies to the existing environmental concerns caused by dangerous pollutant emissions have also emerged. Hydrogen energy systems are effective, with the potential to improve the environment and ensure long-term sustainability [4]. Hydrogen is increasingly looked at as a more viable clean transportation and energy storage solution due to its abundance [3]. As a result, demonstration activities, research, and development in sustainable energy systems are in high demand. The 3S strategy (Source-System-Service) must be met for these systems which include energy and material resources, systems for converting and distributing energy, and energy carriers [5]. But before hydrogen can be completely marketed detailed study and analysis are required to thoroughly understand its advantages and disadvantages [6]. Hydrogen is the most eco-friendly fuel, with a heating value thrice that of petroleum [7]. However, because it is not naturally occurring, processing with various energy and material resources is essential [8]. Consequently, the cost of producing hydrogen is rather high, around thrice the cost of fossil fuels [9,10].

Hydrogen is widely recognized as an important component with immense potential in national as well as international platforms [3]. The transportation industry being one of the largest global energy consumers, needs a transition to smarter energy systems and hydrogen is an excellent contender for ensuring the industry's long-term sustainability [11]. Great optimism has backed the concept of low-cost clean hydrogen as a feasible replacement to fossil fuels focusing on fuel cell applications in transportation [3]. When utilized in fuel cells, it is efficient as fuel and generates just water as a by-product. Another advantage is that its storage may be in little quantities. The application of these energy systems in the transportation sector could strengthen its link to power energy sectors [12].

Hydrogen has several applications in process industries. Hydrogen gas is abundantly used in refineries for a variety of chemical processes and it has a big global market (projected market value of $154.74 billion by 2022 compared to $115.25 billion in 2017). The familiarity of the industry with hydrogen and hence the manufacturing, storage, and transport infrastructure is already in place, offering a suitable starting point for the development of better energy systems [13]. Hydrogen, on combustion, produces only water vapor. Because it dissipates rapidly into the surroundings, the risk of spilling or pooling is non-existent [14–16]. The chemical energy of hydrogen per unit mass (142 MJ) is substantially high when compared with any other hydrocarbon fuel, but it possesses a very low energy content by volume (4 times less than that of

gasoline) and burns much quicker. Natural gas, oil, and coal are currently the cheapest hydrogen sources and are hence primarily used to meet current demand [3]. A shift to green hydrogen is of utmost importance.

Hydrogen storage is a crucial component of a hydrogen system, particularly in large-scale production. It is critical to have a durable and fault-free storage system if the present and future needs of the hydrogen energy market are to be met [12]. The current hydrogen storage systems are either made of metal (predominantly aluminum and steel), polymers, composites, or a combination. There are many associated problems such as weight, volume, weight-to-volume ratio of the storage system, and most important of all, Hydrogen Embrittlement (HE). It usually occurs in storage systems made of metals, specifically steel, because the hydrogen molecule is very small in size and has high mobility (it travels at the speed of sound). Materials impermeable to other gases are susceptible to hydrogen permeation due to the peculiar features of hydrogen [17]. Various factors are known to affect HE and can limit its applications. A critical hydrogen concentration, stress level, and the type of the material affect HE. As the strength of the material (here, steel) increases, so does its susceptibility to embrittlement [18].

High Strength Steels (HSS) are preferred because of their high yield strength, high reliability, and the ability to reduce weight by using thinner materials. There are several different ways to improve the resistance of HSS to HE and to address other concerns. Hydrogen impermeable materials or Hydrogen Permeation Barriers (HPBs) and material-based storage can be employed to reduce the steel's susceptibility to hydrogen permeation and trapping. Several studies have focused on these techniques. However, even with a lot of developments in the field, it is difficult to store hydrogen effectively in HSS storage systems. It is therefore vital to come up with efficient storage materials and methods to enhance the properties of the current hydrogen storage systems.

Methods of hydrogen storage

Storage is crucial to energy systems [12]. Research is being carried out on a grander scale to produce materials that are safe, reliable, small, and cost-effective for application in fuel cell technology. To bring it from the point of manufacture to the point of consumption, hydrogen must be packaged, transported, and stored. There are several challenges associated with hydrogen storage such as low efficiency, long refueling times, and short life span of the materials used. To be suitable for transportation, it is necessary to make hydrogen denser in terms of energy. Storage is the fundamental technological issue for a successful hydrogen economy. Unfortunately, establishing a cost-efficient technique of storage has proven to be an insurmountable hurdle thus far [13].

Hydrogen storage applications can have two categories, stationary and mobile. Stationary systems are mostly used on-site at the location of manufacture or usage, as well as stationary power generation. Mobile systems are used to transport the hydrogen from a location of storage to a location of usage or to utilize hydrogen in a vehicle. When compared with fossil fuels, hydrogen has a low energy density by volume ($9.9\ MJ/m^3$ LHV (Lower Heating Value)), and this could necessitate exceptionally bulky storage tanks. To overcome this, a minimum of one of the following qualities must be present during storage: high pressure, low temperature, or the use of a substance that draws a significant number of hydrogen molecules [12]. HSSs could provide several solutions to current design issues. The present energy storage systems can be categorized into several subclasses. In the gaseous or liquid phases, hydrogen can be stored in its pure, molecular form. These constitute the only way of storing hydrogen on a large scale at present [2]. Different methods of hydrogen storage are shown in Fig. 1.

Hydrogen as a compressed gas

The storage of pressurized gaseous hydrogen in high-pressure tanks is known as compressed hydrogen storage (up to 68.9476 MPa). This approach is advantageous for fuel storage as it allows the fuel to be stored compactly while maintaining its energy efficiency [19–21]. Various standards govern a vessel's design, production, use, and maintenance [22,23], along with specific safety guidelines [24].

When the pressure of the gas is increased, the energy density by volume improves. Although the technique is simple, the procedure is inefficient in terms of volume and gravimetry [25,26]. Storage compartments and compressors (pressure vessels) required to reach the storage pressure are the two essential elements of a compressed hydrogen gas

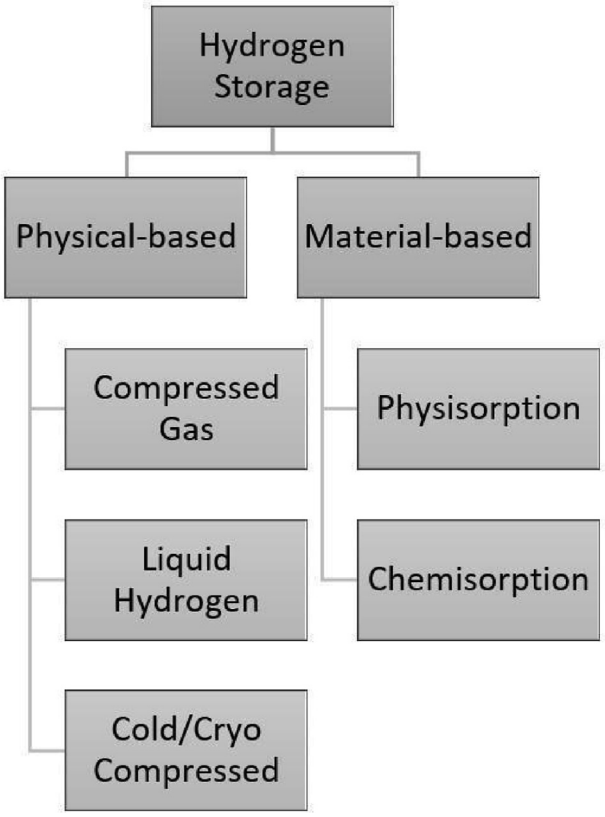

Fig. 1 – A chart depicting physical and material based methods of storing hydrogen [12].

storage system [2]. Large quantities of hydrogen gas are normally not stored at pressures over 10 MPa in aboveground containers and 20 MPa in underground storage facilities due to material characteristics and operating expenses [27]. The attainable hydrogen storage densities are restricted by the storage pressures: at 10 MPa and 20 °C, the density of hydrogen gas is roughly 7.8 kg/m^3. Due to low hydrogen density and large specific volumes, substantial investment costs are required. A lower storage pressure, on the other hand, necessitates less compression effort and consequently cheaper operational expenses [28,29].

In pressure vessels, hydrogen can be stored in four different ways. Type I is a pressure vessel that is entirely made of metal. This is the most common, least expensive, and heaviest variety, weighing about 1362 kg/m^3. They are usually built of steel or aluminum and can hold pressures up to 50 MPa. A steel vessel with a glass fiber composite overwrap is known as Type II. The structural load is distributed evenly between steel and composite materials. These vessels are about 50% more expensive to manufacture than the first type but are 30–40% lighter. The pressure tolerance of this type is the greatest. A complete composite wrap with a metal liner is categorized under Type III. The structure of the composite (carbon fiber composite) carries the majority of the structural load, while the liner (aluminum) functions as a seal. The metal liner withstands about 5% of the mechanical stress. Even though its reliability has been proven at working pressures up to 45 MPa, it still fails aging tests at 70 MPa. This offers a weight of 340.5–454 kg/m^3, around half that of Type II, but at twice the price. Type IV is made of composite materials and a non-metal liner. The liner is usually made of a polymer, for example, High-Density Polyethylene (HDPE). The structural load is sustained by carbon fiber/carbon-glass composites here. Although this style is the lightest, it is still very expensive. It can, however, endure pressures up to 100 MPa [12]. The four types of vessels are illustrated in Fig. 2.

There is an additional Type V vessel that is completely made of composite with no liner. Its initial design was 20% lighter than Type IV vessels and operated at 1.37 MPa, which is appreciably less than the storage pressures required for significant quantities of hydrogen [12].

In general, HE affects metallic materials in contact with hydrogen, particularly steel, resulting in mechanical property degradation and premature cracking. It is caused by the dissolution of H atoms and the formation of a trap (stress corrosion cracking). Industry and academia have made significant attempts to mitigate this problem by acquiring a better knowledge of the mechanisms responsible for HE, improved alloy manufacture, component assembly, and proper mechanical testing [30]. The drawback of using only steel is that it is too heavy for mobile applications. On the other hand, using only composites is very expensive. As mentioned earlier, combinations of both are also used. The materials typically used are carbon fiber and nylon-6, as they are neither poisonous nor hazardous to the environment. High pressure, on the other hand, is always dangerous [31]. Therefore, better materials need to be developed to endure high pressures along with being durable. HE resistant HSS could potentially be this material.

Liquid hydrogen storage

Pure hydrogen's density can be increased by compression. Additionally, it can be increased by liquefaction. Liquefaction is advantageous in the sense that it allows for the achievement of very high storage densities even at atmospheric pressure: saturated liquid hydrogen has a density of 70 kg/m^3 at 0.1 MPa [32]. Liquid hydrogen has predominantly been examined as a medium for delivering hydrogen, where its density (comparatively higher than compressed gas) is a major asset [33].

Liquifying hydrogen requires extremely low temperatures (−250 °C). The complexity and cost of doing so have motivated researchers to seek alternative liquid carriers with more reasonable storage conditions. Liquid Organic Hydrogen Carriers (LOHCs) and ammonia require less stringent conditions than liquid hydrogen, resulting in reduced anticipated costs for transport and storage. Consequently, hydrogen supply chains are now being actively developed with these carriers as the basis [34].

Liquefaction takes time and energy, and as much as 40% of the energy content might be lost along the way, whereas compressed hydrogen storage loses about 10% of the energy. As a result, for storage and distribution on a medium or large scale, such as trucking and intercontinental hydrogen

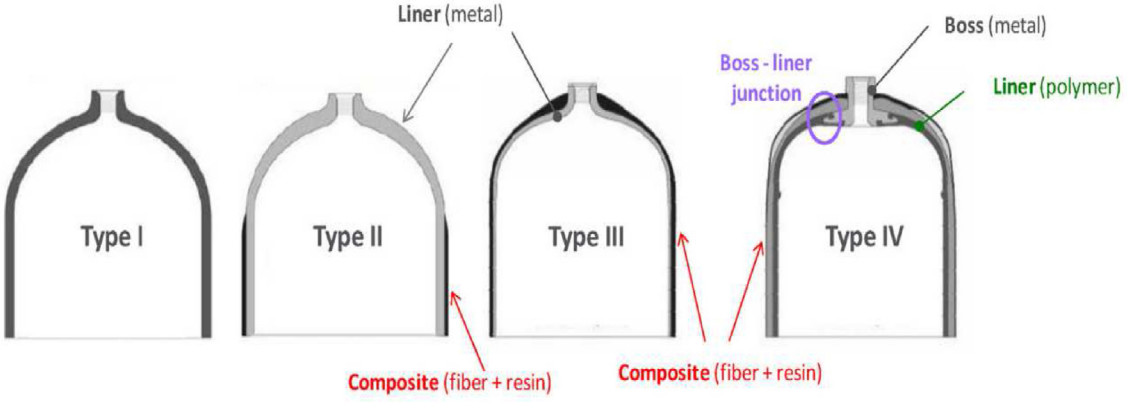

Fig. 2 – Front sectional view of different types of pressure vessels used for storing hydrogen. Various layers that enhance the properties of the vessels are highlighted [30].

shipping, LOHC is usually used. Cryogenic tankers can typically transport five times the volume of gas tube trailers used for compressed hydrogen [12]. The demand for liquid hydrogen vessels for storage and transport is rising for accommodating the future growth of the liquid hydrogen sector. As a result, cryogenic materials and their properties are critical.

Currently, stainless steel and aluminum are preferred due to their corrosion resistance, weldability, and low-temperature performance. However, steel's low-temperature mechanical properties need to be improved. Aluminum, along with being a lightweight metal, has got better formability, weldability, and superior corrosion resistance. Titanium has also been considered as it is strong and possesses low-temperature characteristics. However, it is expensive and therefore not used much. Future investigation into the materials used for liquid hydrogen storage will primarily focus on the following areas: (a) creating a database of mechanical properties of traditional low-temperature materials (stainless steel, titanium alloy, aluminum alloy) in the liquid hydrogen temperature range, (b) developing new high performance and less expensive low-temperature materials, and (c) basic fiber reinforced composite theory and technology research [35].

Cold/cryo-compressed storage

Cryo-compressed hydrogen is a cryogenic gas with a supercritical temperature. Gaseous hydrogen is compressed at around −233 °C where liquefaction does not occur. It is known to be a reliable option when it comes to storage and safety. High storage density, rapid and effective refilling, and a great degree of safety owing to the presence of a vacuum enclosure are all advantages of cryo-compressed storage. It is critical to explore this technology in research and development activities since it has the potential to be widely employed. The availability and cost of infrastructure, however, will continue to be major concerns [12].

Cryogenic storage has a capital cost of $20 to $400 per kilogram. Cryogenic storage is superior in the long run, although compressed storage is desirable for the short-term [36,37]. The approach has good volumetric and gravimetric capacities, but the boil-off problem, heat transfer, long-term storage, and energy costs associated with liquefaction require further investigation [13].

Liquid and gaseous hydrogen can be transported through pipelines both on road and in the ocean. It can also be transported as metal hydrides; however, it is limited to short distances and small quantities. The pipeline may range up to several kilometers with operating pressures between 1 and 3 MPa. Interactions of hydrogen with the pipeline material at high working pressures are still not completely known, especially when pressure cycling is taken into account. High pressures and pressure cycling have an impact on material durability. Transmission lines are primarily made of steel and polyethylene. To prevent steel pipeline embrittlement, coatings are very essential [38].

Material-based hydrogen storage

Material-based hydrogen storage has recently been proposed as an option that could be very significant in the long run [11]. In this method, hydrogen is linked to the base material either through molecules of H_2 on the interior surfaces being taken up by physisorption, like in porous carbon and Metal-Organic Frameworks (MOFs), or by chemical bonding, like in simple metal hydrides, borohydrides, and ammonia borane [39]. Gravimetric and volumetric capacities, working range of temperature, the heat of absorption/desorption, reversibility, and cost are a few parameters that influence material-based hydrogen storage [40].

Physisorption uses lower energy of binding (4–10 kJ mol^{-1}) and is bound by van der Waals forces which are weak. On the other hand, chemisorption uses higher energy of binding (50–100 kJ mol^{-1}) and involves the hydrogen molecule being dissociated on the surface, after which hydrogen atoms diffuse into the metal host lattice. Physisorption is easier to manage than chemisorption as low interaction energy allows reversibility. In addition to this, it has quick adsorption-desorption rates [41]. Rapid kinetics and complete reversibility allow the long lifespan of a cycle and fast refueling times in technological applications, which is why the study of physisorption in materials is gaining importance. The use of traditional porous materials like activated carbons and zeolites to store hydrogen by physisorption has a long history. The amount of surface area that H_2 molecules have access to determines their maximum storage capacity. As a result, gravimetric capacities tend to obey Chahine's rule, which says that hydrogen uptake at 77 K and pressures exceeding 2 MPa is around 1 wt% H_2 per 500 m^2g^{-1} of surface area.

Super-activated and porous carbon-based materials with a high surface area have previously been tested but the research stagnated roughly 20 years ago [34]. Porous-material-based storage systems can provide good-capacity and reliable storage. MOFs and porous carbon compounds are recognized to have the maximum potential of all porous materials [42,43]. This approach will result in a large surface area, low hydrogen binding energy, rapid charge-discharge kinetics, and reduced material costs. Light weight carrier materials, low temperature, and high-pressure operation, and low gravimetric and volumetric hydrogen density are a few challenges associated with this approach [44]. Physical sorption technologies are still in their early stages of development, as all studies are carried out on a small scale and the performance is not up to the mark.

Reversible metal hydrides are well-known under chemisorption [12]. These are metal hydrides (MgH_2) and complex hydrides ($NaAlH_4$, $LiAlH_4$, $LiBH_4$, $NaBH_4$, etc.) [45–55]. Complex hydrides made up of light elements like sodium (Na) and lithium (Li) have received much interest as storage materials [56]. The process of physisorption and chemisorption is depicted in Fig. 3.

The major challenges associated with chemisorption are similar to that of physisorption, along with improving charge-discharge kinetics and minimizing the generation of undesirable gases during desorption.

In the case of LOHCs, the chemical interaction with hydrogen-lean molecules (released through catalytic dehydrogenation) facilitates hydrogen storage [58]. The store and release processes are free of carbon, and the unconsumed carrier liquid can be reused, making these storage devices desirable. These carriers have a low storage pressure in

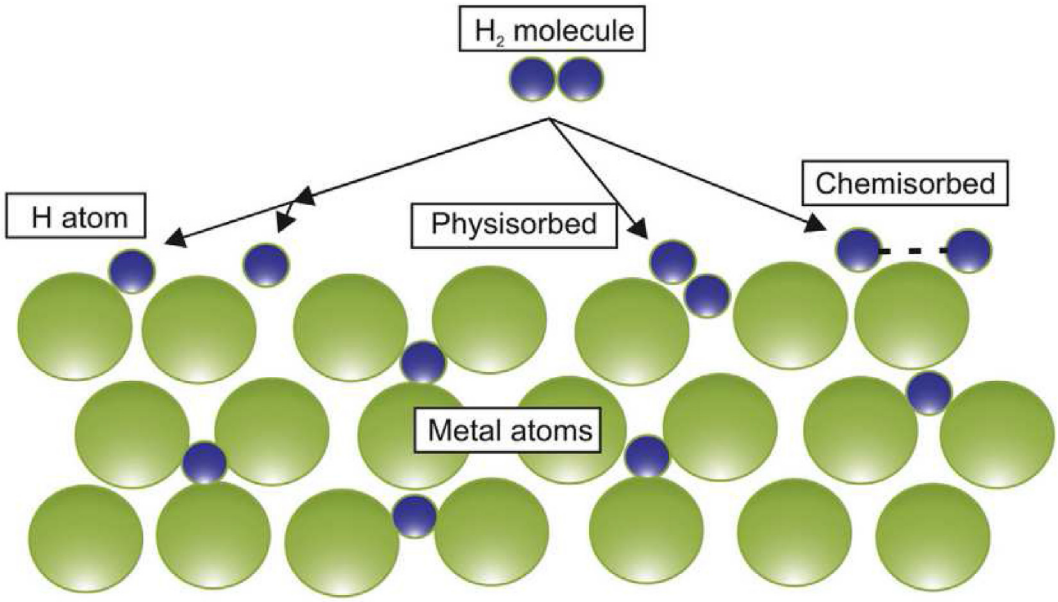

Fig. 3 – Schematic representation highlighting the formation of metal hydrides. Mechanisms such as physisorption and chemisorption are depicted [57].

addition to being non-toxic and non-corrosive. However, there is a problem with a low hydrogen storage capacity which limits the use of LOHCs for various applications [59]. The different methods of physical and chemical storage along with their maximum storage capacities are listed in Table 1.

The weight of the system is relatively unimportant in stationary applications like grid energy storage, whereas in mobile applications, lightweight materials are desirable to decrease the curb weight of the vehicle so that the fuel consumption is reduced. Niche applications are being designed to capitalize on the advantages of each class of materials. For a long system life cycle, excellent reversibility is essential, and the price per kWh of storage capacity ought to be minimal as these systems are typically built for storing huge amounts of energy [39].

Due to the beneficial qualities of two-dimensional (2D) materials like high aspect ratios, outstanding mechanical stiffness, and exceptional thermal conductivity, they have significant potential as useful hydrogen storage materials [60–64]. The use of MXenes, layered structures, and their composites has been investigated from many domains (e.g., EMI shielding, electro-CO2 reduction, catalyst, hydrogen evolution, supercapacitor, batteries, and catalysis) [60,65–74].

For the synthesis of the majority of MXenes, HF is a commonly used etchant. Other etchants for MXene production, however, have been suggested due to its toxicity [75]. Alkaline etching techniques were used to create MXenes in addition to HF and fluoride salt etching techniques [76]. The Bayer process, which is used to refine bauxite, served as an inspiration for the fluorine-free production of MXene. Multilayer MXene sheets with a purity of ~92 wt% were created using this technique. This fluorine-free alkali-etching technique can be used to avoid the release of HF. However, heating concentrated alkaline solutions (like NaOH) at high temperatures and pressures under hydrothermal conditions results in safety concerns. This issue was addressed by proposing a new

Table 1 – Storage capacities of various physical and chemical methods of hydrogen storage [12].

	Storage method (material-based)	Highest reported storage capacity (% wt)
Physical	Carbon Materials	8
	Zeolites	9.2
	Glass Capillary Arrays	10
	Glass Microspheres	14
Chemical	Ammonia Borane	19.4
	Metal Hydrides	12.6
	Alanates	9.3
	Formic Acid	4.4
	Carbohydrates	14.8
	Liquid Organic Hydrogen Carriers	7.2

tetramethylammonium hydroxide (TMAOH) etchant [77]. As delamination agents, a variety of other organic bases including hydrazine, urea, choline hydroxide, and n-butylamine were subsequently tested. These organic molecules intercalate into layers of the MXene flakes, which readily delaminate when sonicated or shaken [78,79]. By dispersing MAX powders in dimethyl sulfoxide (DMSO) with the use of high-energy mechanical milling, the synthesis of few-layer MXenes was also accomplished [80]. Fast electron transport (with decreased charge transfer resistance) and Na + diffusion have been demonstrated in the produced few-layer MXene sheets, which is advantageous for electrochemical applications [81]. Like graphene, MXenes were also synthesized using electrochemical techniques. In this procedure, MAX phases were electrochemically etched to produce MXenes [82].

MXenes can be considered for hydrogen storage applications because transition metals like titanium have already been employed to increase the hydrogen storage capacity of carbon-based materials [83,84]. The presence of transition

Table 2 – Hydrogen storage capacities of various MXene-based materials [89].

Material	E_{ad} (eV/H or eV/H_2)	Total hydrogen storage capacity (wt %)	Reference
Ti_2C	5.027	8.6	[90]
MgH_2-10 wt% $(Ti_{0.5}V_{0.5})_3C_2$	–	6.5	[91]
Cr_2C	0.96	7.6	[92]
Ti_2N	3.63	8.55	[93]
Ti_2NO_2	0.142	5.38	[93]
Ti_2NF_2	0.137	5.176	[93]
$Ti_2N(OH)_2$	0.153	5.31	[93]
MgH_2-5 wt% $Nb_4C_3T_x$	–	3.50	[94]
NaH/Al-8 wt% Ti_3C_2	–	4.9	[95]
$LiBH_4$ + 40 wt% Ti_3C_2	–	5.37	[96]
Sc_2C	4.307	9.0	[97]

metals in MXenes can be effective in the storage of hydrogen via Kubas-type interaction [85,86].

Because it can supply binding energy in between chemisorption and physisorption, the Kubas-type binding interaction is crucial for hydrogen storage. The Kubas-type interaction is consistent with the lengthening of H–H bond without breakage with an electron donation [87]. The unoccupied σ* anti-bonding orbital of the H_2 molecule receives a π-back donation from a filled transition metal (D-orbital) at the same moment. Many attempts have been made to raise the binding energy between hydrogen and host material in order to create Kubas-type interaction (for example, metal ornamentation on sorption materials) [83,88]. However, the creation of such materials, which store hydrogen using Kubas-type interaction, is still difficult [89]. Table 2 shows the hydrogen storage capacities of various MXene-based materials.

Although MXene-based materials offer immense opportunities in hydrogen storage applications due to their better capacities, their usefulness in this area has only seldom been evaluated so far [90]. MXene materials are capable of achieving reversible hydrogen storage of 6.4 wt% and the maximal gravimetric hydrogen storage of up to 8.8 wt%. The MXene-based materials are particularly promising for reversible hydrogen storage applications, as evidenced by their excellent hydrogen storage capacity [89].

Hydrogen embrittlement in high-strength steels

HE is characterized by the generation and propagation of cracks that eventually lead to the degradation of mechanical properties like ductility, tensile strength, and fatigue strength. It may even cause the failure of the material [98]. Metallic materials such as precipitation hardening (PH) steels, low-alloy steels, super alloys, and aluminum alloys are the ones that get most affected by this phenomenon. HE is predominantly seen in high-strength materials such as steel where there is a reduction of strength due to the interaction with the hydrogen atoms [99]. The hydrogen atoms get trapped within the metal and then breach the material, ultimately generating cracks. Two kinds of fracture occur inside the material; one is an intergranular fracture where the cracks propagate at very high speed, and the other is a *trans*-granular fracture where the fracture occurs outside the boundaries of the grain [100].

During hydrogen permeation and trapping, the hydrogen is nascent, not molecular. This phenomenon is reversible as diffusible hydrogen is the cause of embrittlement. The effusion of diffusible hydrogen from steel leads to frothing and stronger steels are more susceptible to HE [101].

Fig. 4 demonstrates the hydrogen-permeation mechanism in solid materials [102]. Given that diffusible hydrogen damages steel, any method that makes hydrogen immobile should help limit this damage. Hydrogen penetrating the steel in trace amounts, usually less than 1 ppm, is drawn to stress fields found near crack tips. As a result, it accumulates and aggravates the fracture process [101].

HSSs are most vulnerable to this phenomenon because of their Ultimate Tensile Strength (UTS) of around 1000 MPa and mechanical properties that make them useful for several domains such as space, nuclear research, hydrogen storage (operated at high pressures), transportation, etc. [100]. The advancement of HSSs is seen in high manganese steel and martensitic advanced high-strength steels (MS-AHSS), but these high Mn steels are prone to HE because of their chemical composition. MS-AHSS is a relatively new kind that has the highest strength amongst steels and is widely used in automobile industries. Therefore, it is also the most susceptible to HE.

There are several factors that are responsible for HE, such as material strength, residual stress, microstructure, pressure, temperature, exposure time, applied strain rate, surface condition of material, hydrogen concentration, heat treatment methods, tensile stresses in-service conditions, etc. [99].

A study showed that the accumulation of hydrogen is directly proportional to the pre-strain conditions of the metal. HE initially decreases with an increase in pre-strain, but with a continued increase of pre-strain, HE also increases [103]. The effects of high-pressure and high-purity hydrogen gas on metals have also been studied. HE tends to increase with pressure, although it depends on the material [104]. In another study, with the increase in carbon concentration of the metal, HE increased as well. Twinning resulted in hydrogen-enriched locations while slipping resulted in hydrogen dispersion [105].

The microstructure of metallic materials significantly influences hydrogen uptake and trapping. Microstructural changes may occur as a result of fatigue stress, which could explain the observed variance in hydrogen uptake [106]. The factors responsible for HE are shown in Fig. 5.

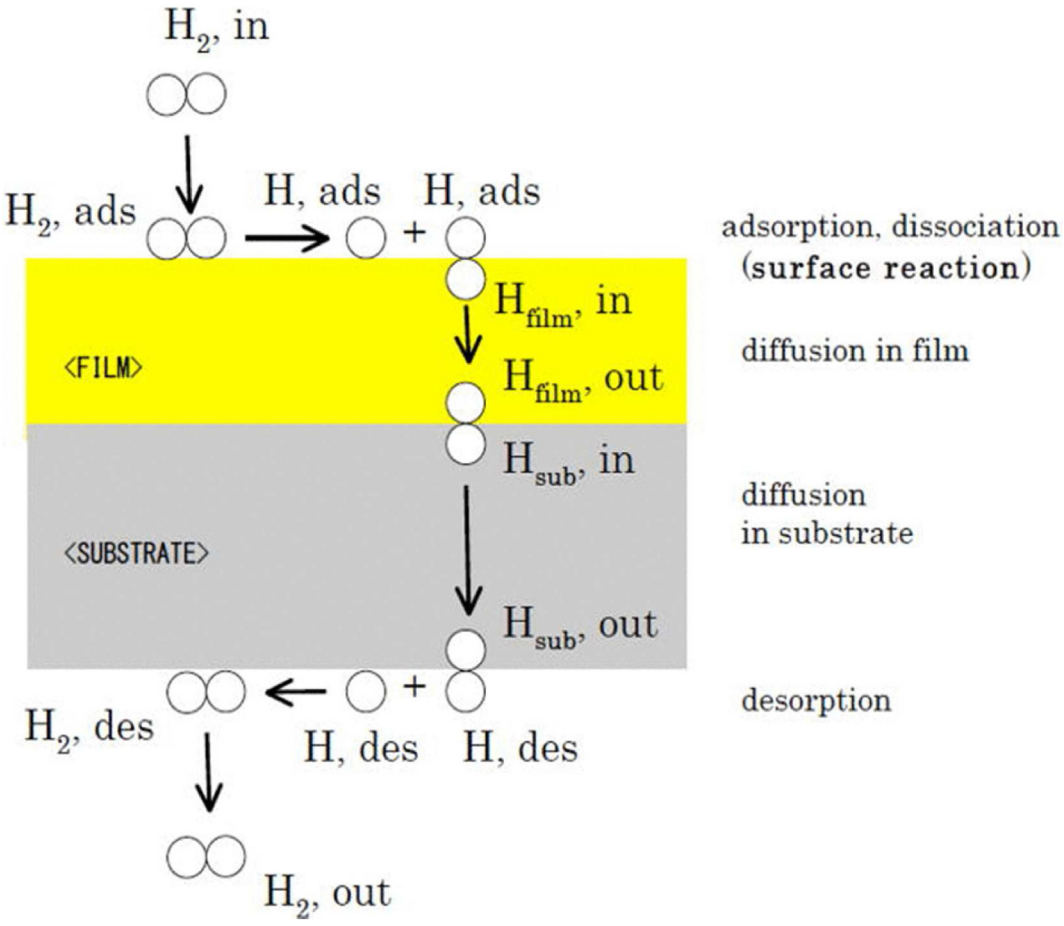

Fig. 4 – Mechanism of hydrogen permeation (absorption, diffusion, desorption) through film and substrate [102].

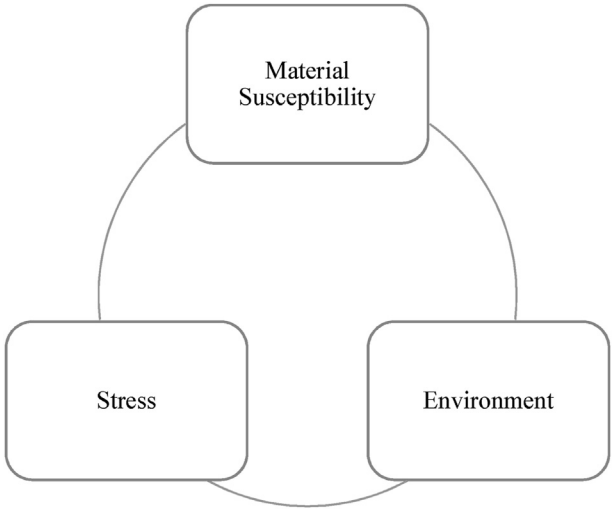

Fig. 5 – The three main factors that are responsible for hydrogen embrittlement [100].

HE is classified into two categories. The first one is subcritical crack growth at a stress level between the threshold stress and the yield stress, which occurs due to the large hydrogen concentration at the tip of the crack leading to embrittlement. Chemical corrosion at the tip initiates this phenomenon. The second one is fracture initiation which takes place at stress somewhere in between the yield stress and the ultimate tensile strength (UTS). This happens if there is sufficient growth in the length of the crack. If the critical crack length is achieved, this fracture occurs below the material's UTS [100]. An intergranular crack caused by HE is illustrated in Fig. 6.

Hydrogen embrittlement mechanisms

The mechanisms through which HE occurs in HSSs are Hydrogen Enhanced Decohesion Mechanism (HEDE), Hydrogen Enhanced Localized Plasticity (HELP), and Absorption Induced Dislocation Emission (AIDE) [107–115].

HEDE is the first established mechanism that concentrates on the change of material properties owing to atomic hydrogen. It is built on the induction of a hydrogen atom at the tip of the crack, lowering the material's cohesive strength. Upon the attainment of the critical crack tip opening displacement (CTOD), decohesion occurs. When atoms of hydrogen are present everywhere on the surface of the material and certain stresses are applied, hydrogen atoms diffuse inside the material, lowering the material's cohesive strength at the tip and causing a cleavage-like fracture. Reduction in a material's cohesive strength leads to the surface energy being reduced, resulting in lowering the fracture stress, causing the

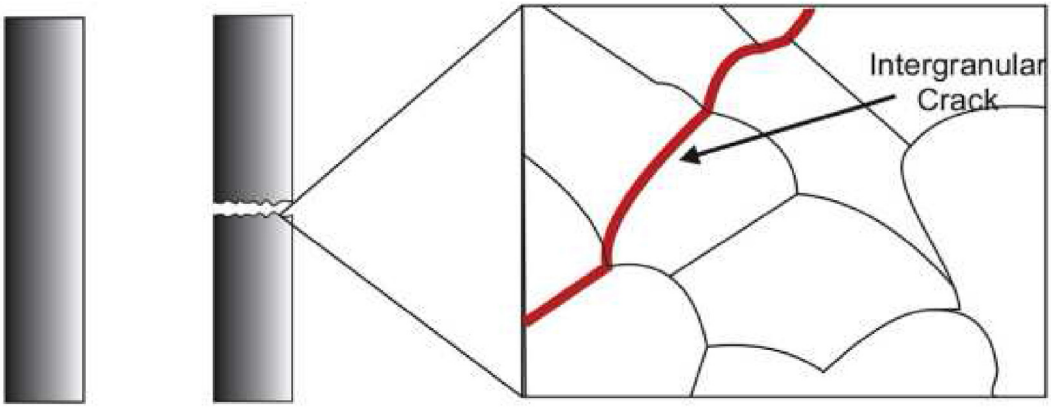

Fig. 6 – Depiction of intergranular crack caused by hydrogen embrittlement [57]. A magnified view of the crack at molecular level can be seen.

fracture to occur below the permissible value. The sole drawback of this approach is the ability to measure the cohesive force [100].

In HELP, the hydrogen atoms accumulate around the crack tip and this enhances dislocation motion. As a result, dislocation maneuverability improves and these dislocations act as bearers of plastic deformation in the metal lattice. Plastic deformation depends on the material's hydrogen clustering, microstructure, or intensity of the applied stress. Fractographic analysis was used to assess the microstructure qualities of the material [99]. However, no clear connection was established between the anticipated or suggested HELP model and the actual embrittlement mechanism [116]. Based on the amount of hydrogen, the microstructure, and the stress intensity at the crack tip, several fracture modes, such as intergranular, *trans*-granular, and quasi-cleavage may be observed. It was determined by fractography that it has stronger local plastic deformation and lower macroscopic ductility. With the action of the hydrogen atom, the activation energy for dislocation motion is lowered, as is the activation

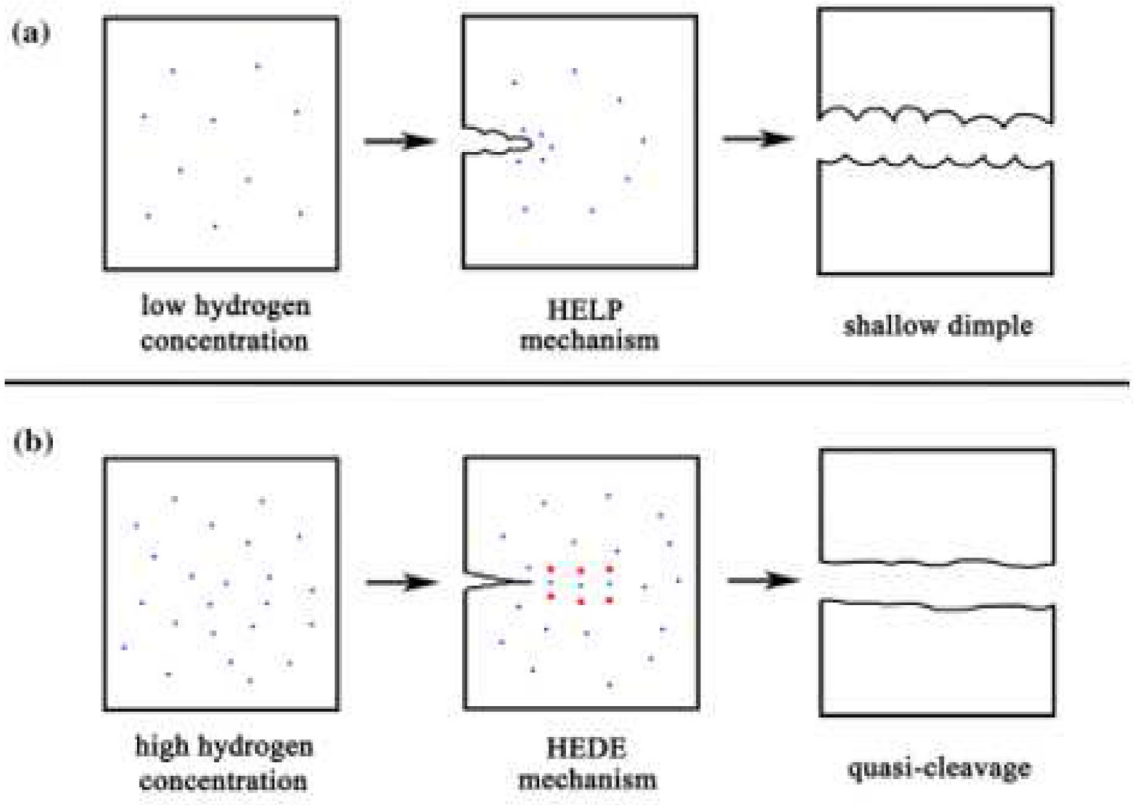

Fig. 7 – Schematic representation of hydrogen embrittlement highlighting two mechanisms, (a) Hydrogen Enhanced Decohesion Mechanism (HEDE) and (b) Hydrogen Enhanced Localized Plasticity (HELP) [122].

area [110,112,117–121]. HELP contains a variety of structures, including pure materials, alloys, FCC, BCC, and HCP types [110].

AIDE (depicted in Fig. 8) is a combination of HEDE and HELP (depicted in Fig. 7). Near the fracture tip, the solute hydrogen atoms are adsorbed. Because of solute hydrogen atom-induced dislocations close to the fracture tip, the interatomic connections and cohesive strength of the material are weakened via the HEDE process. The HELP mechanism accelerates the propagation of cracks and the creation of micro voids through dislocation [123].

It is important to study how crack growth happens in inert (non-embrittling) conditions for ductile materials to comprehend why dislocation emission leads to embrittlement. With little to no dislocation emission at the crack tips, it appears that egress of dislocations is the primary mechanism by which ductile cracks evolve. Because interatomic bonding at fracture tips is inherently strong, dislocation emission from crack tips is likely challenging in inert or air settings. Only a small number of dislocations precisely intersect crack tips to induce crack advance – most produce only blunting or contribute to the strain ahead of cracks. Therefore, to cause crack growth via micro void coalescence (MVC), large strains are required ahead of the fractures. As a result, the fracture surfaces develop large dimples with smaller dimples inside of them. The coalescence of large voids involves the nucleation and growth of small voids between large voids. Consequently, small dimples arise within large dimples. High dislocation activity leads to crack growth when hydrogen adsorption weakens interatomic connections and encourages dislocation emission from fracture tips. This is because dislocation emission on suitably sloped slip planes induces both crack advance and crack opening. As a result, when AIDE develops, lower strains result in the coalescence of cracks with voids, and smaller dimples are generated on the fracture surfaces. Ductile fracture results in stretched and challenging-to-resolve small dimples within large dimples, whereas AIDE/MVC produces dimples that are smaller (and shallower) than in ductile fracture [110].

Hydrogen-Enhanced Strain-Induced Vacancy (HESIV) is another type of HE mechanism. The results of thermal desorption spectrometry (TDS) in iron and low alloyed ferritic steels were used to develop HESIV. Below 200 °C, where the dislocation density was not thought to vary, it was seen that the rate of hydrogen desorption decreased. It was proposed that the elimination of vacancies could be the cause for such a reduction. Further research revealed that the presence of hydrogen increased the density of strain-induced voids inferred from the TDS data, supporting the HESIV process. The results of positron annihilation spectroscopy (PAS) supported this finding after observing an increase in the mean positron lifetime in the presence of pre-charged hydrogen. As a result of the hydrogen-induced vacancies, premature fracture could occur close to the high stress/strain concentrators, encouraging the creation of vacancy clusters and very small nano-sized voids.

In a different investigation, a group carefully analyzed the fracture surfaces of embrittled and hydrogen-charged ferritic pipeline steels using scanning electron microscopy (SEM). They discovered that the brittle facet that was usually visible at a lower magnification had a “mottled” dark-bright contrast on the nanoscale. A detailed examination of the conjugate fracture surfaces and the findings of atomic force microscopy (AFM) supported the suggestion that this contrast was with relation to nano dimples. The existence of nano dimples was then evidence of the HESIV model's functionality. It will be challenging to obtain more direct experimental evidence for this mechanism, because it is difficult to directly characterize hydrogen and vacancies using currently available tools [124].

Most HSSs possess microstructure spots locally distinguished by very high gradients in the local mechanical stress. This is the primary cause of embrittlement. These spots can

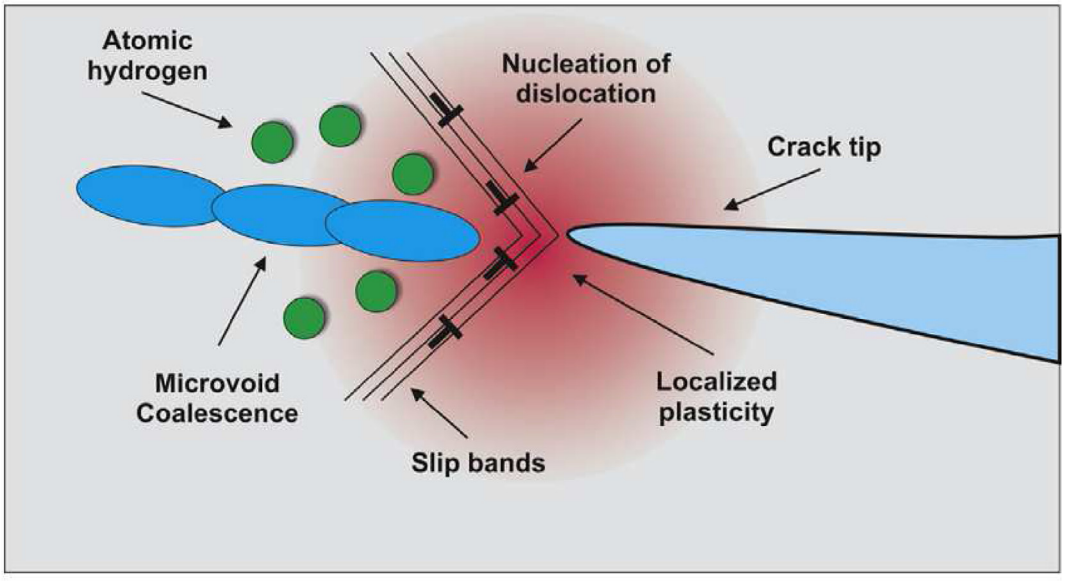

Fig. 8 – Schematic representation of Absorption Induced Dislocation Emission (AIDE) mechanism [57]. Formation of microvoid coalescence and slip bands at the tip of the crack can be seen.

occur at hetero-interfaces between dissimilar components or in areas with a lot of dislocations, resulting in a lot of micro-mechanical contrast. Either way, hydrogen often accumulates in the most neuralgic parts of these complex microstructures and triggers HE mechanisms [123].

Analysis of microstructure

Advanced high-strength steels (AHSS) are alloys that often have very complex and hierarchical microstructures made up of ferrite, austenite, bainite, or martensite matrix, as well as duplex or multiphase mixes of these elements supplemented with precipitates. Because of this complexity, establishing trustworthy and mechanism-based microstructure–property correlations is difficult [123]. AHSSs are extremely vulnerable to HE, as indicated by the significant loss of load-bearing capability even when only a few parts per million of hydrogen are present. This obstructs their continued development and implementation, potentially putting an end to worldwide weight-reduction attempts in the automotive industry [124].

A study looked into the role of microstructure in dual-phase (DP), quenched and partitioned (Q&P), and twinning-induced plasticity (TWIP) steels. The hydrogen influence altered the fracture mode at UTS, preventing subcritical crack formation at lower stresses. In DP steels, the fractures started in the hard martensite and/or at the interfaces of ferrite and martensite. In Q&P steels, the fractures started in the martensite and/or at the interfaces of retained austenite and martensite. In TWIP steels, the fractures started at mechanical twins. Tempering DP and Q&P steels may improve their resistance to hydrogen [125].

The martensite phase is important in defining MS-AHSS HE susceptibility. Because martensite is naturally brittle, it has a poor tolerance for embrittlement. Furthermore, martensite has a high defect density (i.e., dislocation and boundary defects), which effectively traps hydrogen. Hydrogen trapping can cause hydrogen defect interactions, leading to quick initiation and propagation of fracture. The bulk of dislocations, which are naturally present in the martensite phase, appears to have the most impact on MS-AHSS HE susceptibility. This is due to the ability of the dislocations to effectively trap hydrogen and create hydrogen-enhanced localized plastic deformation, resulting in a reduction in yield strength. Localized plasticity in the fracture site provided indirect evidence of the participation of dislocations in producing hydrogen-accelerated fracture. Prior austenite grain boundaries (PAG), block and lath borders, and other boundary or interface defects come in second to dislocations in terms of contributing to hydrogen sensitivity in MS-AHSS. The presence of trans granular, intergranular, and quasi-cleavage fractures on the shear fracture surface indicated boundary-related fractures, and they were also the key markers of brittle fracture. The hydrogen trapped in the PAG, block, and lath borders may be linked to the formation of these fractures. Trans granular, intergranular, and quasi-cleavage fractures could all have been caused by dislocation-based hydrogen fracture mechanisms. These types of fractures are most likely caused by a combination of both causes. Volume defects like voids, porosity, phase discontinuity, and inclusions operate as stress concentrators, increasing the steel's hydrogen sensitivity [121].

Beyond the specific embrittling methods, the fact that most of these steels possess local microstructure areas with extremely significant gradients in local mechanical stress is the most important factor. These can happen at hetero-interfaces between dissimilar materials or in areas with a lot of dislocations, resulting in a large amount of micro-mechanical contrast. In either of the cases, these are the most neuralgic areas in these complex microstructures, where hydrogen accumulates and HE is triggered. As a result, appropriate defensive measures for making these steels more resistant to HE must include strategies to strengthen and mitigate sharp stress peaks in the microstructures, as well as the development of denser oxide surface layers with reduced hydrogen diffusion and take-up rates [123].

In the determination of a material's and alloy's HE susceptibility, analyzing the microstructure is critical. SEM and Transmission Electron Microscopy (TEM) are common analytical techniques for establishing a material's internal microstructure, as well as the effect of hydrogen on the internal microstructure and material characterization. This is crucial when studying fracture structures like micro voids, dimples, and fisheyes. The most effective and recommended method is TEM. To address the difficulties of SEM, TEM uses high magnification and resolution. A million times magnification and nanoscale resolution are possible with TEM. TEM can be used to collect information on morphology and topography. This microscope also provided crystallographic data. However, one complication that has arisen while working with TEM is the need for sample preparation. The sample must be electron transparent for TEM imaging, and the sample thickness must be less than 100 nm [100].

Knowing the mechanism of fracture growth, microstructure, and its progression rate is critical in assessing the susceptibility of a material to hydrogen permeation and trapping. Material selection and how they can be made impermeable are more significant for reducing or even preventing HE as a whole [99].

Prevention of hydrogen embrittlement and hydrogen impermeable materials

Prevention of HE

HE produced by hydrogen's contact with metallic material has always been a common method of deterioration of metallic components. In industries such as petrochemical, automobile, and aerospace, hydrogen-induced mechanical characteristics, and corrosion resistance are important parameters related to the service safety of HSSs. HE is a major stumbling block to metal structural materials operating safely. The presence of hydrogen in steel and other metals can cause many structural failures, including hair-line crack development, embrittlement, increased brittleness, and corrosion susceptibility. It is therefore critical to find efficient protection solutions [126]. To prevent HE, the material design must be appropriate. In a recent study, the baking process (heat treatment process) was carried out to remove absorbed

hydrogen. The elevated temperatures help hydrogen diffuse out [124].

HSSs can be protected from HE by knowing the real hydrogen source and the mechanism responsible for it. Materials that act as a barrier should be selected properly as coatings and the hydrogen diffusion should be lowered. If adequate adhesion, coating thickness, and defect-free coatings are given, the chances of embrittlement are reduced [100].

Internal hydrogen and external hydrogen are the two most common types of hydrogen sources. Internal hydrogen is generated during smelting, welding, and other material preparation techniques. External hydrogen is the one generated during service due to corrosion, pickling/plating, and exposure to environments containing hydrogen gas and hydrogen sulfide (H_2S). As a result, two approaches to HE prevention can be considered. One is the application of surface treatments. Coating and modification of surfaces are involved in the prevention of external embrittlement. The other method involves altering the material microstructure by adding or removing the required alloy components as well as alloy microstructure optimization [98].

Coatings and Hydrogen Permeation Barriers

Incorporating metal alloys into the base material and offering a layer of protection on top is another way of avoiding HE. Vacuum-deposited coating, organic coating, and mechanical plating are some coating processes. The use of effective inhibitors is also significant [100,101].

There exist only a handful of materials fit to be HPBs, with incredibly low bulk hydrogen solubility and diffusivity, which may have been measured using outdated, low-sensitivity methods. Moreover, the majority of HPB-suitable deposition processes produce films with a statistically distributed number of tiny flaws. Dust particles and/or other random occurrences are frequently the cause of pinholes and fissures while the film grows. Another flaw in the HPB structure is the presence of nano-channels between columns that are oriented in the direction of film production, significantly reducing the Permeation Reduction Factor (PRF). Consequently, in addition to intrinsic material properties, it is a must for a successful HPB to possess a very low defect rate, which is a huge technological challenge. Low solubility is a more relevant parameter than low diffusivity in contributing to a high PRF value in fusion-related HPBs, implying that low solubility is more of a key attribute that leads to a high PRF value.

Today, hard coatings are made using a few ceramic materials with exceptionally little hydrogen solubility and permeability. Many of these are not even available in bulk form as technical materials. A couple of them have been identified as HPBs. Although oxides are constantly found on most metal surfaces, their hydrogen permeability varies substantially depending on the atomic structure. Two of the most well-known oxides with significantly different characteristics are dense alumina, whose hydrogen permeability is very low, and nano-porous iron oxide, which is practically transparent to hydrogen. Many oxides used as HPBs can be formed over irregular geometrical patterns simply by subjecting the metal to air at elevated temperatures, which is one of their most appealing properties [127]. In a particular study, chromium oxide (Cr_2O_3) was established to be a strong contender as an HPB when generated on top of pure chromium, which had been examined using the very same method in the past. Its penetration effectiveness at 700 and 800 °C was indicated by a PRF of 1000 in comparison with pure chromium substrate [128]. The main element on the surface of stainless steel that keeps the base metal beneath it from oxidizing is Cr_2O_3 [127]. Recently, erbium oxide (Er_2O_3) has been recognized as a good HPB. The bulk hydrogen characteristics of this material are unknown, although its HPB efficiency is reportedly comparable to that of alumina. At temperatures ranging from 600 to 800 °C, filtered arc discharge deposited a thick HPB with a PRF of around 800–1000 [129].

Nitrides, because of their broad applicability as hard coatings and decorating films, where the critical criteria are dense packing and homogeneity, have been acknowledged as efficient HPBs. Accomplished outcomes on nitrides as HPBs are difficult to review since they are frequently described in a way that is not as clear or detailed as the PRF. A good example of well-run experimentation is the report on the evaluation of boron nitride (BN) coatings on stainless steel. BN capacity as an HPB is unfortunately not displayed in a method that can be converted to a PRF value [127]. If titanium is present in high quantities, it can diminish the susceptibility of a hot stamped boron steel to HE by generating titanium carbide (TiC) in the material.

Coatings of niobium and graphene can also protect materials against HE. The reduced graphene oxide (rGO) layer offers an adequate barrier and is stable after hydrogen charging in one study. Due to increased diffusion length along with the formation of a C–H bond during hydrogen charging, this was possible [100]. Table 3 indicates the efficiencies of different HPBs.

Table 3 – Efficiency of dielectric materials, recently recognized as HPBs, expressed as Pf at 400 °C [127].

	PRF	d_s mm	d_f μm	P_s x10^{-11} molH_2/s/m/$Pa^{0.5}$	P_f x10^{-18} molH_2/s/m/$Pa^{0.5}$
Al_2O_3	1000	0.5	1	1.30	25.9
Cr_2O_3	1000	1.6	10*	0.017	0.72*
Cr_2O_3/Al_2O_3	3500	0.5	1	1.30	7.41
Er2O3	1000	0.5	1	1.30	25.9
Er_2O_3	1000	0.5	1.3	1.30	33.7
SiO_2	1	0.15	0.2	0.13	1711
BN	100	0.1	1.5	0.13	193
TiN	100	0.1	1.5	0.13	193
TiN	1100	0.35	1.7	0.13	5.7
TiN	1000	0.1	1.7	0.13	21.8
TiAlN	6800	0.35	1.7	0.13	0.92
TiAlN	20000	0.5	5	1.30	6.5
SiN	2000	0.5	0.5	1.30	6.5
WN	38	0.5	2.3	1.30	1570
CrWN	100	0.5	4.4	1.30	1140
CrN	117	0.5	2.6	1.30	576
Cr2N	236	0.5	2.2	1.30	241
AlCrN	350	0.5	4.5	1.30	333
ZrN	4600	0.5	1.4	1.30	7.9
TiC	10	0.1	1	0.27	2750
TiN + TiC	100	0.5	1 + 0.25	1.30	324

* Thickness of Cr_2O_3 is assumed due to lack of information.

There are also a variety of techniques used for applying coatings to protect HSS from HE [130]. In general, because of the strong interaction between atoms in good HPBs, a deposition approach that incorporates ion-aided deposition produces superior outcomes than methods that do not require an electric or magnetic field. The capacity to cover enormous regions and complex three-dimensional surfaces is the next major concern. This is a flaw present in all approaches that use electric and magnetic fields. On the other hand, oxidation at high temperatures, which produces great HPB uniformity, can only be used on a small number of substrate candidates, resulting in a poor PRF. Furthermore, the substrate must be able to tolerate high temperatures, which is essential for the oxidation process to produce a dense structure [127].

In a study, chemical vapor deposition (CVD), electroplating discharge (EPD), electrolysis, gas diffusion, plasma diffusion, high-velocity oxygen fuel (HVOF), magnetically enhanced plasma ion plating system, plasma vapor deposition, and ion beam sputter were used to apply these coatings on HSSs followed by characterization and mechanical testing. The shortening of the life cycle caused by HE was also examined [130]. Table 4 shows different types of coatings and the techniques used to deposit them on a substrate.

Graphene is the most suitable choice for reducing the HE in HSSs. It possesses a thin coating of carbon atoms with special features [132–134]. Its chemical inertness allows it to be used in a variety of operating conditions. It is also stable at temperatures up to 400 °C and reduces oxidation of the substrate due to its hydrophobic property [135], which is attributable to its non-polar covalent double bonds that prohibit hydrogen atoms from interacting with water [130]. However, when stainless steel is coated by CVD, graphene coating can reduce its corrosion resistance. Due to its enormous volume, low cost, and room-temperature processing abilities, rGO has superseded graphene. The electrophoretic-deposition approach is one of the most cost-effective ways to produce rGO on stainless steel (EPD) [136]. In a study, during the charging condition, rGO coating boosted hydrogen resistance by forming C–H bonds and increasing diffusion length. As a result, rGO can operate as a barrier to hydrogen permeation and resist HE at the same time [130]. The use of EPD to deposit rGO on stainless steel is depicted in Fig. 9.

Another study found that a niobium layer applied on API 5CT P110 steel using thermal spraying with HVOF served as a barrier of protection against hydrogen ingestion. The trapping process in the layer was regulated by the defects in it, primarily holes and oxides. Thermal spraying has proven to be a viable solution to HE in components [137].

The effects of electroplating Zn, Cu, Ni, Al, PVD-Ti-DLC, and NiP coatings, as well as diffusion layers of oxygen, nitrogen, and carbon, on HE susceptibility, were examined. Carbon and nitrogen were discovered to be effective diffusion layers in reducing hydrogen diffusion. When working on the hydrogen atmosphere, it was discovered that very little work has been done on tensile and ductility improvement. But it was found that diffusion layers of Ni and C reduced the propagation of cracks [130].

MoS_2 coating acts as a good barrier to hydrogen adsorption or permeability, preventing hydrogen damage. When this coating was applied to iron, it was observed that the hydrogen absorption energy on the iron surface was enhanced, which means that it was effective in inhibiting permeation. MoS_2 can efficiently prevent hydrogen adsorption and penetration by forming an S–H bond, as was discovered by the characterization of hydrogen-adsorbed MoS_2/Fe(111). The work function also increased when the coating was applied, implying that the iron was made significantly corrosion-resistant. Multiple layers of MoS_2 or a thin film, based on the protective performance of monolayer MoS_2, are projected to have a greater hydrogen prevention effect due to additional hydrogen diffusion barriers. Because producing a high-quality monolayer MoS_2 film on a big scale on steel is still difficult, coating with many layers of MoS_2 film may be a better option [138].

In Ni– MoS_2 coatings, by adjusting the concentration of MoS_2 in the electrodeposition bath, the amount of MoS_2 integrated into coatings may be effectively regulated. As the MoS_2 concentration rises from 0 to 8 kg/m^3, the coating's MoS_2 content rises from 0 to 7.08 wt%. Adding MoS_2 to Ni deposits also reduces the compressive residual stresses in coatings, but the opposite is true if too much MoS_2 is added. MoS_2 can greatly improve the microstructure of composite coatings, which is advantageous for boosting the coatings' ability to retard the permeation of hydrogen. Meanwhile, the addition of MoS_2 can significantly increase the adhesive strength of coatings on the substrate [139].

Table 4 – Different coatings and coating methods for the prevention of hydrogen embrittlement [131].

Coating material	Coating type	Deposition technique	Thickness μm	Hardness, HB/HV[a]	Adhesion acc [HF]	Remarks
Al	On top	Electroplating	22	15–25 HB	4	Globular structure
Cu	On top	Electroplating	2	50–110 HB	1	Thin coating with pin load
Ni	On top	Electroplating	12	510 HV	1	Ni adhesion coating
Zn	On top	Electroplating	11	92 HV	2	Ductile zinc coating
NiP	On top	Electroless	10	550 HV	2	Amorphous NIP-type coating
Ti-DLC	On top	Physical Vapor Deposition (PVD)	3	1440 HV	1	Ti adhesion coating
Carbon	Diffusion	Gas diffusion	25	1225 HV	1	Long-term gas diffusion
Nitrogen	Diffusion	Gas diffusion	500	300 HV	1	Small-term gas diffusion
Oxygen	Diffusion	Plasma Diffusion	1	1200 HV	2	Oxidizing at −550 °C

[a] HV was calculated using the formula HB = 0.95 HV

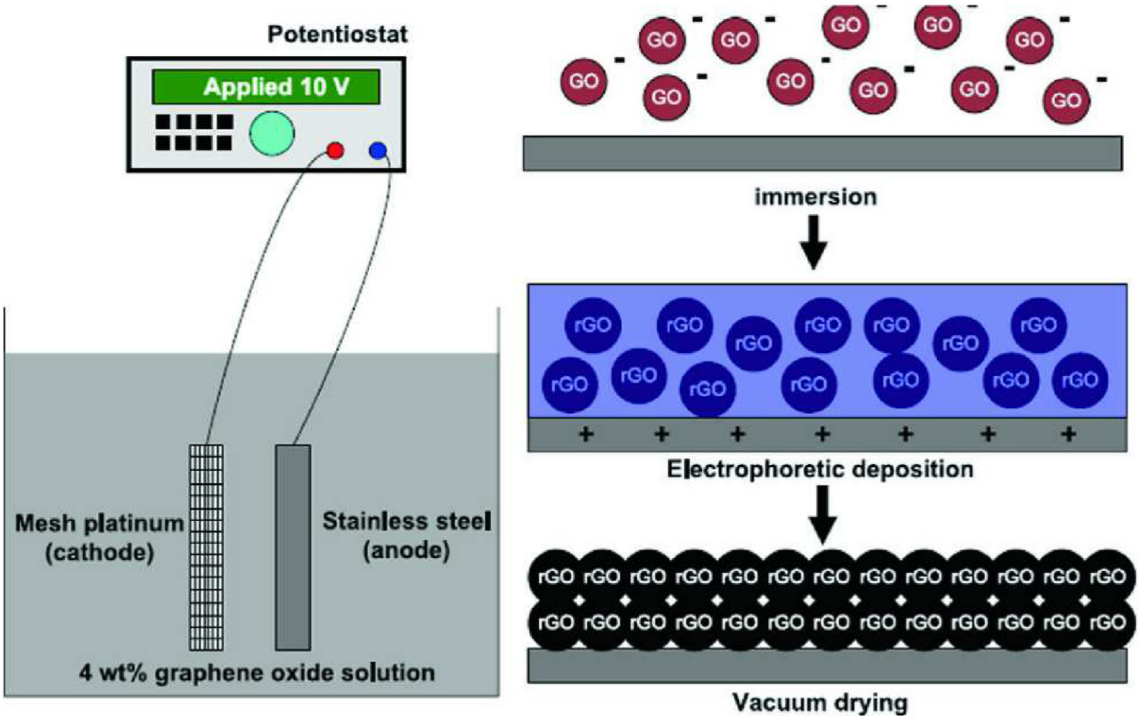

Fig. 9 – Illustration of rGO deposition on stainless steel using electroplating discharge [136]. Different steps of the electroplating mechanism are indicated.

Ni coatings can further enhance the effect of coating on delaying hydrogen penetration, resulting in a lower hydrogen permeation current density in samples, by adding MoS_2 or graphene. More intriguingly, increasing the amount of graphene is marginally superior to increasing the amount of MoS_2, as evidenced by a greater reduction in the current density of hydrogen permeation and a lower hydrogen diffusion coefficient in Ni-graphene. Therefore, if the inclusion of inert and impermeable graphene into other metallic deposits with lower hydrogen diffusion coefficients is implemented in the future, it will be of higher importance [140].

It has been demonstrated that two-dimensional (2D) materials provide good hydrogen resistance and corrosion prevention [141]. A novel class of graphene-like-nanomaterials named MXenes has recently piqued interest in the domains of energy storage, catalysis, tribology, and membrane separation technology [142,143]. Due to its ease of use, ability to precisely regulate the film thickness, and nearly pollution-free nature, spin coating is frequently used to prepare 2D MXene coatings [144]. The MXene is a potential hydrogen barrier coating due to its molecular sieve [145–147] and hydrogen storage [148] properties. It gives steel resistance to both corrosion and hydrogen permeation [149].

When the arc ion plating method was used to coat AISI 316L austenitic stainless steel (substrate), it was discovered that TiC, TiN, and TiAlN coatings along with the multi-layered TiAlN/TiMoN were dense and effective hydrogen barriers. At a test temperature of 573 K, the hydrogen permeabilities of TiAlN-coated, TiN-coated, and TiAlN/TiMoN multi-layered coating samples were 1/100, <1/100, and 1/1000 of the uncoated substrate, respectively. In the tests, coatings having fine crystal grains were proven to be incredibly effective as hydrogen barriers. Many crystal grain boundaries are thought to have existed in these coatings, acting as hydrogen diffusion barriers. As per previous studies on hydrogen forms in materials, lattice defects (atom vacancies, dislocations, and crystal grain borders), impurity atoms, precipitates, inclusion interfaces, and voids are all examples of hydrogen trap sites.

Future research must focus on determining which coating flaws affect hydrogen barriers, and also the extent to which this effect exists. At hydrogen trapping locations, hydrogen diffusion mobility is restricted. At crystal grain boundaries and film interfaces, hydrogen atoms that permeate the coating are considered to be securely trapped. The hydrogen permeability of the TiAlN/TiMoN multi-layered coating was also found to be the least. The findings of this work indicated that the crystal grain boundaries and film interfaces functioned as hydrogen diffusion barriers in fine crystal grain and multi-layered coatings, effectively minimizing hydrogen permeability and that these hydrogen barrier coatings were more efficient when these particular microstructures were involved [150]. Fig. 10 illustrates the hydrogen traps present at the grain boundaries as well as the layer interfaces.

Most of these techniques can be extended to HSSs. More research needs to be done, especially concerning how these coatings and techniques are related to the microstructure of the HSS. For example, appropriate strategies for making these steels more resistant to HE should involve strengthening and mitigating steep stress peaks in the microstructures, as well as the development of denser oxide surface layers with relatively low hydrogen diffusion and take-up rates [123]. It is also postulated that microstructure development of coatings will become increasingly essential in the future [150].

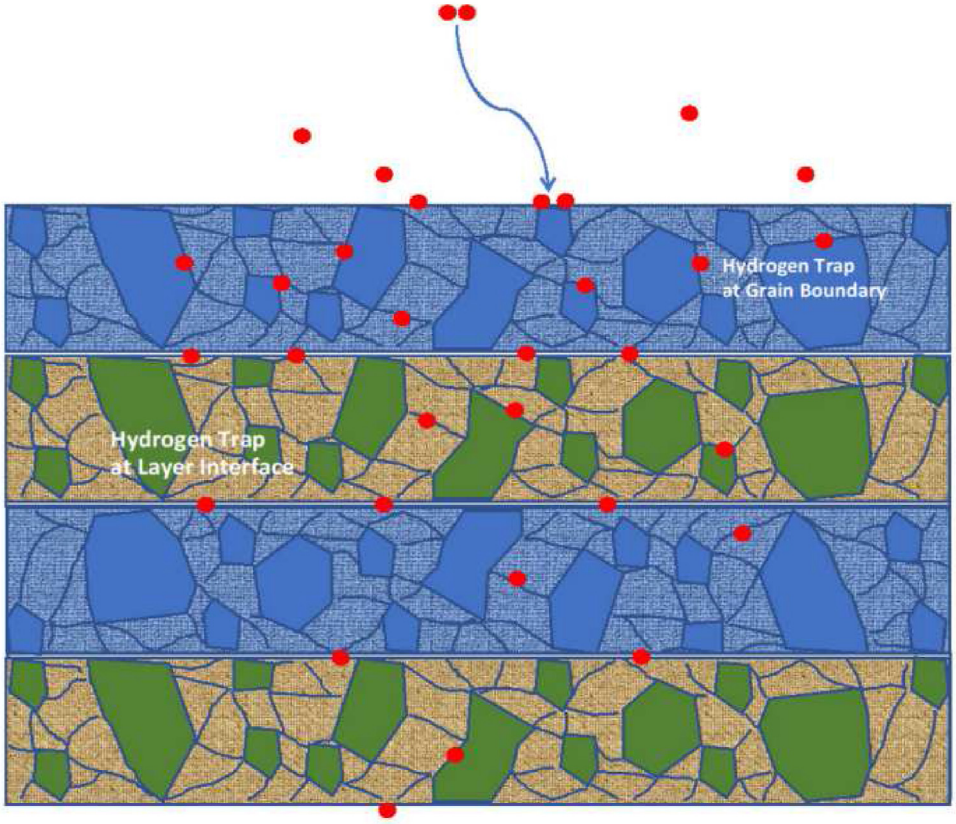

Fig. 10 – Hydrogen traps present at the crystal grain boundaries and film interfaces of multi-layered coatings [150].

Conclusion

There are plenty of approaches currently being employed for the storage of hydrogen in various forms such as compressed gas, liquid hydrogen, cryo-compressed storage, and material-based storage. However, these have many limitations in terms of applications due to the problems associated with energy efficiency and the properties of the materials being used. The development of next-generation materials is crucial and timely if the transport and storage of hydrogen is to be made more efficient.

It can be concluded that, HSSs are promising for hydrogen storage and should be encouraged because of their high yield strength, high reliability, and ability to reduce weight. HE is the main reason for HSSs being avoided in the hydrogen storage systems that are being used today as it leads to premature cracking and resulting in material failure. Knowing the mechanism of fracture growth, microstructure and its progression rate is critical in assessing the susceptibility of a material to hydrogen permeation and trapping.

Many coatings have not been particularly tried on HSSs yet, but multi-layered coatings could significantly increase their resistance to HE. For the effective application of coatings, thorough knowledge of the relation between microstructure and hydrogen permeation is of immense importance so that the correct coating material and deposition technique can be identified. Material selection and how they can be made impermeable to hydrogen are more significant for reducing or even preventing HE as a whole.

The modification of HSSs using several materials and techniques could help shift the industries of many domains to hydrogen technology and combat the numerous environmental catastrophes faced by the planet especially climate change due to the use of fossil fuels. It is therefore crucial to continue working in this area if more energy-efficient and economical hydrogen storage systems are to be designed for a green future.

Declaration of competing interest

The authors declare that they have no known competing financial interests or personal relationships that could have appeared to influence the work reported in this paper.

REFERENCES

[1] Sazali N. Emerging technologies by hydrogen: a review. Int J Hydrogen Energy 2020;45:18753–71. https://doi.org/10.1016/j.ijhydene.2020.05.021.
[2] Andersson J, Grönkvist S. Large-scale storage of hydrogen. Int J Hydrogen Energy 2019;44:11901–19. https://doi.org/10.1016/j.ijhydene.2019.03.063.
[3] Noussan M, Raimondi PP, Scita R, Hafner M. The role of green and blue hydrogen in the energy transition—a technological and geopolitical perspective. Sustain Times 2021;13:1–26. https://doi.org/10.3390/su13010298.

[4] Dincer I. Green methods for hydrogen production. Int J Hydrogen Energy 2012;37:1954–71. https://doi.org/10.1016/j.ijhydene.2011.03.173.
[5] Dincer I, Acar C. Smart energy systems for a sustainable future. Appl Energy 2017;194:225–35. https://doi.org/10.1016/j.apenergy.2016.12.058.
[6] Salvi BL, Subramanian KA. Sustainable development of road transportation sector using hydrogen energy system. Renew Sustain Energy Rev 2015;51:1132–55. https://doi.org/10.1016/j.rser.2015.07.030.
[7] Acar C, Dincer I. Experimental investigation and analysis of a hybrid photoelectrochemical hydrogen production system. Int J Hydrogen Energy 2017;42:2504–11. https://doi.org/10.1016/j.ijhydene.2016.03.099.
[8] Ehret O, Bonhoff K. Hydrogen as a fuel and energy storage: success factors for the German Energiewende. Int J Hydrogen Energy 2015;40:5526–33. https://doi.org/10.1016/j.ijhydene.2015.01.176.
[9] Acar C, Ghosh S, Dincer I, Zamfirescu C. Evaluation of a new continuous type hybrid photo-electrochemical system. Int J Hydrogen Energy 2015;40:11112–24. https://doi.org/10.1016/j.ijhydene.2014.12.036.
[10] AlRafea K, Fowler M, Elkamel A, Hajimiragha A. Integration of renewable energy sources into combined cycle power plants through electrolysis generated hydrogen in a new designed energy hub. Int J Hydrogen Energy 2016;41:16718–28. https://doi.org/10.1016/j.ijhydene.2016.06.256.
[11] Acar C, Dincer I. The potential role of hydrogen as a sustainable transportation fuel to combat global warming. Int J Hydrogen Energy 2020;45:3396–406. https://doi.org/10.1016/j.ijhydene.2018.10.149.
[12] Moradi R, Groth KM. Hydrogen storage and delivery: review of the state of the art technologies and risk and reliability analysis. Int J Hydrogen Energy 2019;44:12254–69. https://doi.org/10.1016/j.ijhydene.2019.03.041.
[13] Niaz S, Manzoor T, Pandith AH. Hydrogen storage: materials, methods and perspectives. Renew Sustain Energy Rev 2015;50:457–69. https://doi.org/10.1016/j.rser.2015.05.011.
[14] Züttel A. Materials for hydrogen storage. Mater Today 2003;6:24–33. https://doi.org/10.1016/S1369-7021(03)00922-2.
[15] van den Berg AWC, Areán CO. Materials for hydrogen storage: current research trends and perspectives. Chem Commun 2008:668–81. https://doi.org/10.1039/B712576N.
[16] Borgschulte A, Schlapbach L, Zuttel A. Hydrogen as a future energy carrier. Wiley-VCH Verlag; 2008.
[17] Elberry AM, Thakur J, Santasalo-Aarnio A, Larmi M. Large-scale compressed hydrogen storage as part of renewable electricity storage systems. Int J Hydrogen Energy 2021;46:15671–90. https://doi.org/10.1016/j.ijhydene.2021.02.080.
[18] Trautmann A, Mori G, Oberndorfer M, Bauer S, Holzer C, Dittmann C. Hydrogen uptake and embrittlement of carbon steels in various environments. Materials 2020;13:1–16. https://doi.org/10.3390/MA13163604.
[19] Dillon AC, Heben MJ. Hydrogen storage using carbon adsorbents: past, present and future. Appl Phys 2001;72:133–42. https://doi.org/10.1007/s003390100788.
[20] Schlapbach L, Züttel A. Hydrogen-storage materials for mobile applications. Nature 2001;414:353–8. https://doi.org/10.1038/35104634.
[21] Satyapal S, Petrovic J, Read C, Thomas G, Ordaz G. The U.S. Department of energy's national hydrogen storage project: progress towards meeting hydrogen-powered vehicle requirements. Catal Today 2007;120:246–56. https://doi.org/10.1016/j.cattod.2006.09.022.
[22] Barilo NF, Weiner SC, James CW. Overview of the DOE hydrogen safety, codes and standards program part 2: hydrogen and fuel cells: emphasizing safety to enable commercialization. Int J Hydrogen Energy 2017;42:7625–32. https://doi.org/10.1016/j.ijhydene.2016.04.070.
[23] Ohi JM, Rossmeissl N. Hydrogen codes and standards: an overview of US DOE activities. In: Proc. 16th world hydrog. Energy Conf.; 2006.
[24] Rivkin C, Burgess R, Buttner W. Hydrogen technologies safety guide. 2015. https://doi.org/10.2172/1169773. United States.
[25] Bogdanović B, Schwickardi M. Ti-doped alkali metal aluminium hydrides as potential novel reversible hydrogen storage materials1Invited paper presented at the International Symposium on Metal–Hydrogen Systems, Les Diablerets. J Alloys Compd 1997;253–254:1–9. https://doi.org/10.1016/S0925-8388(96)03049-6. August 25–30, 1996, Switzerland.1.
[26] Li Y, Yang RT. Significantly enhanced hydrogen storage in Metal–Organic Frameworks via spillover. J Am Chem Soc 2006;128:726–7. https://doi.org/10.1021/ja056831s.
[27] Wolf E. Chapter 9 - large-scale hydrogen energy storage. In: Moseley PT, Garche J, editors. Electrochem. Energy storage renew. Sources grid balanc. Amsterdam: Elsevier; 2015. p. 129–42. https://doi.org/10.1016/B978-0-444-62616-5.00009-7.
[28] Witkowski A, Rusin A, Majkut M, Stolecka K. Comprehensive analysis of hydrogen compression and pipeline transportation from thermodynamics and safety aspects. Energy 2017;141:2508–18. https://doi.org/10.1016/j.energy.2017.05.141.
[29] Hua TQ, Ahluwalia RK. Alane hydrogen storage for automotive fuel cells – off-board regeneration processes and efficiencies. Int J Hydrogen Energy 2011;36:15259–65. https://doi.org/10.1016/j.ijhydene.2011.08.081.
[30] Barthelemy H, Weber M, Barbier F. Hydrogen storage: recent improvements and industrial perspectives. Int J Hydrogen Energy 2017;42:7254–62. https://doi.org/10.1016/j.ijhydene.2016.03.178.
[31] Rivard E, Trudeau M, Zaghib K. Hydrogen storage for mobility: a review. Materials 2019;12. https://doi.org/10.3390/ma12121973.
[32] Storage of Pure Hydrogen in Different States. Hydrog. Storage Technol., John Wiley & Sons, Ltd; n.d., pp. 97–170. https://doi.org/https://doi.org/10.1002/9783527649921.ch4.
[33] Cardella U, Decker L, Klein H. Roadmap to economically viable hydrogen liquefaction. Int J Hydrogen Energy 2017;42:13329–38. https://doi.org/10.1016/j.ijhydene.2017.01.068.
[34] Hirscher M, Yartys VA, Baricco M, Bellosta von Colbe J, Blanchard D, Bowman RC, et al. Materials for hydrogen-based energy storage – past, recent progress and future outlook. J Alloys Compd 2020;827. https://doi.org/10.1016/j.jallcom.2019.153548.
[35] Qiu Y, Yang H, Tong L, Wang L. Research progress of cryogenic materials for storage and transportation of liquid hydrogen. Metals 2021;11. https://doi.org/10.3390/met11071101.
[36] Padro C, Putsche V. Survey of the economics of hydrogen technologies. 2010. https://doi.org/10.2172/12212.
[37] Amos W a. Costs of storing and transporting hydrogen. Other Inf PBD 27 Jan 1999; PBD 27 Jan 1999; PBD 27 Jan 1999 1999:Medium: ED; Size: vp.
[38] Abohamzeh E, Salehi F, Sheikholeslami M, Abbassi R, Khan F. Review of hydrogen safety during storage, transmission, and applications processes. J Loss Prev Process Ind 2021;72:104569. https://doi.org/10.1016/j.jlp.2021.104569.

[39] Chanchetti LF, Leiva DR, Lopes de Faria LI, Ishikawa TT. A scientometric review of research in hydrogen storage materials. Int J Hydrogen Energy 2020;45:5356–66. https://doi.org/10.1016/j.ijhydene.2019.06.093.
[40] Sandrock G. A panoramic overview of hydrogen storage alloys from a gas reaction point of view. J Alloys Compd 1999;293–295:877–88. https://doi.org/10.1016/S0925-8388(99)00384-9.
[41] Ren J, Musyoka NM, Langmi HW, Mathe M, Liao S. Current research trends and perspectives on materials-based hydrogen storage solutions: a critical review. Int J Hydrogen Energy 2017;42:289–311. https://doi.org/10.1016/j.ijhydene.2016.11.195.
[42] Xia Y, Yang Z, Zhu Y. Porous carbon-based materials for hydrogen storage: advancement and challenges. J Mater Chem 2013;1:9365–81. https://doi.org/10.1039/C3TA10583K.
[43] Zhu Q-L, Xu Q. Metal–organic framework composites. Chem Soc Rev 2014;43:5468–512. https://doi.org/10.1039/C3CS60472A.
[44] Zhang F, Zhao P, Niu M, Maddy J. The survey of key technologies in hydrogen energy storage. Int J Hydrogen Energy 2016;41:14535–52. https://doi.org/10.1016/j.ijhydene.2016.05.293.
[45] Ouyang L, Liu F, Wang H, Liu J, Yang X-S, Sun L, et al. Magnesium-based hydrogen storage compounds: a review. J Alloys Compd 2020;832:154865. https://doi.org/10.1016/j.jallcom.2020.154865.
[46] Ali NA, Idris NH, Din MFM, Mustafa NS, Sazelee NA, Halim Yap FA, et al. Nanolayer-like-shaped MgFe2O4 synthesised via a simple hydrothermal method and its catalytic effect on the hydrogen storage properties of MgH2. RSC Adv 2018;8:15667–74. https://doi.org/10.1039/C8RA02168F.
[47] He T, Cao H, Chen P. Complex hydrides for energy storage, conversion, and utilization. Adv Mater 2019;31:1902757. https://doi.org/10.1002/adma.201902757.
[48] Idris NH, Mustafa NS, Ismail M. MnFe2O4 nanopowder synthesised via a simple hydrothermal method for promoting hydrogen sorption from MgH2. Int J Hydrogen Energy 2017;42:21114–20. https://doi.org/10.1016/j.ijhydene.2017.07.006.
[49] Schüth F, Bogdanović B, Felderhoff M. Light metal hydrides and complex hydrides for hydrogen storage. Chem Commun 2004:2249–58.
[50] Ismail M, Yahya MS, Sazelee NA, Ali NA, Yap FAH, Mustafa NS. The effect of K2SiF6 on the MgH2 hydrogen storage properties. J Magnes Alloy 2020;8:832–40. https://doi.org/10.1016/j.jma.2020.04.002.
[51] Sazelee NA, Yahya MS, Ali NA, Idris NH, Ismail M. Enhancement of dehydrogenation properties in LiAlH4 catalysed by BaFe12O19. J Alloys Compd 2020;835:155183. https://doi.org/10.1016/j.jallcom.2020.155183.
[52] Sazelee NA, Idris NH, Md Din MF, S.Yahya M, Ali NA, Ismail M. LaFeO3 synthesised by solid-state method for enhanced sorption properties of MgH2. Results Phys 2020;16:102844. https://doi.org/10.1016/j.rinp.2019.102844.
[53] Ismail M, Mustafa NS, Ali NA, Sazelee NA, Yahya MS. The hydrogen storage properties and catalytic mechanism of the CuFe2O4-doped MgH2 composite system. Int J Hydrogen Energy 2019;44:318–24. https://doi.org/10.1016/j.ijhydene.2018.04.191.
[54] Ali NA, Yahya MS, Mustafa NS, Sazelee NA, Idris NH, Ismail M. Modifying the hydrogen storage performances of NaBH4 by catalyzing with MgFe2O4 synthesized via hydrothermal method. Int J Hydrogen Energy 2019;44:6720–7. https://doi.org/10.1016/j.ijhydene.2019.01.149.
[55] Yahya MS, Ali NA, Sazelee NA, Mustafa NS, Halim Yap FA, Ismail M. Intensive investigation on hydrogen storage properties and reaction mechanism of the NaBH4-Li3AlH6 destabilized system. Int J Hydrogen Energy 2019;44:21965–78. https://doi.org/10.1016/j.ijhydene.2019.06.076.
[56] Ali NA, Ismail M. Modification of NaAlH4 properties using catalysts for solid-state hydrogen storage: a review. Int J Hydrogen Energy 2021;46:766–82. https://doi.org/10.1016/j.ijhydene.2020.10.011.
[57] Del-Pozo A, Villalobos JC, Serna S. A general overview of hydrogen embrittlement. Curr Trends Futur Dev Membr Recent Adv Met Membr 2020:139–68. https://doi.org/10.1016/B978-0-12-818332-8.00006-5.
[58] Preuster P, Papp C, Wasserscheid P. Liquid organic hydrogen carriers (LOHCs): toward a hydrogen-free hydrogen economy. Acc Chem Res 2017;50:74–85. https://doi.org/10.1021/acs.accounts.6b00474.
[59] Teichmann D, Arlt W, Wasserscheid P. Liquid Organic Hydrogen Carriers as an efficient vector for the transport and storage of renewable energy. Int J Hydrogen Energy 2012;37:18118–32. https://doi.org/10.1016/j.ijhydene.2012.08.066.
[60] Kumar P, Shahzad F, Yu S, Hong SM, Kim Y-H, Koo CM. Large-area reduced graphene oxide thin film with excellent thermal conductivity and electromagnetic interference shielding effectiveness. Carbon N Y 2015;94:494–500. https://doi.org/10.1016/j.carbon.2015.07.032.
[61] Peng L, Fang Z, Zhu Y, Yan C, Yu G. Holey 2D nanomaterials for electrochemical energy storage. Adv Energy Mater 2018;8:1702179. https://doi.org/10.1002/aenm.201702179.
[62] Butler SZ, Hollen SM, Cao L, Cui Y, Gupta JA, Gutiérrez HR, et al. Progress, challenges, and opportunities in two-dimensional materials beyond graphene. ACS Nano 2013;7:2898–926. https://doi.org/10.1021/nn400280c.
[63] Edwards RS, Coleman KS. Graphene synthesis: relationship to applications. Nanoscale 2013;5:38–51. https://doi.org/10.1039/C2NR32629A.
[64] Kumar P, Yu S, Shahzad F, Hong SM, Kim Y-H, Koo CM. Ultrahigh electrically and thermally conductive self-aligned graphene/polymer composites using large-area reduced graphene oxides. Carbon N Y 2016;101:120–8. https://doi.org/10.1016/j.carbon.2016.01.088.
[65] Kong X, Peng Z, Jiang R, Jia P, Feng J, Yang P, et al. Nanolayered heterostructures of N-doped TiO2 and N-doped carbon for hydrogen evolution. ACS Appl Nano Mater 2020;3:1373–81. https://doi.org/10.1021/acsanm.9b02217.
[66] Kong X, Gao P, Jiang R, Feng J, Yang P, Gai S, et al. Orderly layer-by-layered TiO2/carbon superstructures based on MXene's defect engineeringfor efficient hydrogen evolution. Appl Catal Gen 2020;590:117341. https://doi.org/10.1016/j.apcata.2019.117341.
[67] Yang Y, Gao P, Wang Y, Sha L, Ren X, Zhang J, et al. A direct charger transfer from interface to surface for the highly efficient spatial separation of electrons and holes: the construction of Ti–C bonded interfaces in TiO2-C composite as a touchstone for photocatalytic water splitting. Nano Energy 2017;33:29–36. https://doi.org/10.1016/j.nanoen.2017.01.030.
[68] Ren X, Xu F, Peng Z, Chi Q, Li W, Wang J, et al. Boosting visible light driven hydrogen production: bifunctional interface of Ni(OH)2/Pt cocatalyst on TiO2. Int J Hydrogen Energy 2020;45:16614–21. https://doi.org/10.1016/j.ijhydene.2020.04.090.
[69] Yang Y, Sun T, Ma F, Huang L-F, Zeng Z. Superhydrophilic Fe3+ doped TiO2 films with long-lasting antifogging performance. ACS Appl Mater Interfaces 2021;13:3377–86. https://doi.org/10.1021/acsami.0c18444.
[70] Yang Y, Ye K, Cao D, Gao P, Qiu M, Liu L, et al. Efficient charge separation from F– selective etching and doping of

anatase-TiO2{001} for enhanced photocatalytic hydrogen production. ACS Appl Mater Interfaces 2018;10:19633–8. https://doi.org/10.1021/acsami.8b02804.
[71] Cho KY, Yeom YS, Seo HY, Kumar P, Lee AS, Baek K-Y, et al. Ionic block copolymer doped reduced graphene oxide supports with ultra-fine Pd nanoparticles: strategic realization of ultra-accelerated nanocatalysis. J Mater Chem 2015;3:20471–6. https://doi.org/10.1039/C5TA06076A.
[72] Cho KY, Yeom YS, Seo HY, Kumar P, Lee AS, Baek K-Y, et al. Molybdenum-Doped PdPt@Pt core–shell octahedra supported by ionic block copolymer-functionalized graphene as a highly active and durable oxygen reduction electrocatalyst. ACS Appl Mater Interfaces 2017;9:1524–35. https://doi.org/10.1021/acsami.6b13299.
[73] Cho KY, Seo HY, Yeom YS, Kumar P, Lee AS, Baek K-Y, et al. Stable 2D-structured supports incorporating ionic block copolymer-wrapped carbon nanotubes with graphene oxide toward compact decoration of metal nanoparticles and high-performance nano-catalysis. Carbon N Y 2016;105:340–52. https://doi.org/10.1016/j.carbon.2016.04.049.
[74] Kumar P. Ultrathin 2D nanomaterials for electromagnetic interference shielding. Adv Mater Interfac 2019;6:1901454.
[75] Halim J, Lukatskaya MR, Cook KM, Lu J, Smith CR, Näslund L-Å, et al. Transparent conductive two-dimensional titanium carbide epitaxial thin films. Chem Mater 2014;26:2374–81. https://doi.org/10.1021/cm500641a.
[76] Li T, Yao L, Liu Q, Gu J, Luo R, Li J, et al. Fluorine-free synthesis of high-purity Ti3C2Tx (T=OH, O) via alkali treatment. Angew Chem Int Ed 2018;57:6115–9. https://doi.org/10.1002/anie.201800887.
[77] Xuan J, Wang Z, Chen Y, Liang D, Cheng L, Yang X, et al. Organic-base-Driven intercalation and delamination for the production of functionalized titanium carbide nanosheets with superior photothermal therapeutic performance. Angew Chem Int Ed 2016;55:14569–74. https://doi.org/10.1002/anie.201606643.
[78] Naguib M, Unocic RR, Armstrong BL, Nanda J. Large-scale delamination of multi-layers transition metal carbides and carbonitrides "MXenes. Dalton Trans 2015;44:9353–8. https://doi.org/10.1039/C5DT01247C.
[79] Maleski K, Mochalin VN, Gogotsi Y. Dispersions of two-dimensional titanium carbide MXene in organic solvents. Chem Mater 2017;29:1632–40. https://doi.org/10.1021/acs.chemmater.6b04830.
[80] Yang Q, Xu Z, Fang B, Huang T, Cai S, Chen H, et al. MXene/graphene hybrid fibers for high performance flexible supercapacitors. J Mater Chem 2017;5:22113–9. https://doi.org/10.1039/C7TA07999K.
[81] Urbankowski P, Anasori B, Makaryan T, Er D, Kota S, Walsh PL, et al. Synthesis of two-dimensional titanium nitride Ti4N3 (MXene). Nanoscale 2016;8:11385–91. https://doi.org/10.1039/C6NR02253G.
[82] Sun W, Shah SA, Chen Y, Tan Z, Gao H, Habib T, et al. Electrochemical etching of Ti2AlC to Ti2CTx (MXene) in low-concentration hydrochloric acid solution. J Mater Chem 2017;5:21663–8. https://doi.org/10.1039/C7TA05574A.
[83] Yildirim T, Ciraci S. Titanium-Decorated carbon nanotubes as a potential high-capacity hydrogen storage medium. Phys Rev Lett 2005;94:175501. https://doi.org/10.1103/PhysRevLett.94.175501.
[84] Wu M, Gao Y, Zhang Z, Zeng XC. Edge-decorated graphene nanoribbons by scandium as hydrogen storage media. Nanoscale 2012;4:915–20. https://doi.org/10.1039/C2NR11257D.
[85] Chung C, Ihm J, Lee H. Recent progress on Kubas-type hydrogen-storage nanomaterials: from theories to experiments. J Kor Phys Soc 2015;66:1649–55. https://doi.org/10.3938/jkps.66.1649.
[86] Hoang TKA, Antonelli DM. Exploiting the Kubas interaction in the design of hydrogen storage materials. Adv Mater 2009;21:1787–800. https://doi.org/10.1002/adma.200802832.
[87] Skipper CVJ, Hamaed A, Antonelli DM, Kaltsoyannis N. The Kubas interaction in M(ii) (M = Ti, V, Cr) hydrazine-based hydrogen storage materials: a DFT study. Dalton Trans 2012;41:8515–23. https://doi.org/10.1039/C2DT30383C.
[88] Bhattacharya A, Bhattacharya S, Majumder C, Das GP. Transition-metal decoration enhanced room-temperature hydrogen storage in a defect-modulated graphene sheet. J Phys Chem C 2010;114:10297–301. https://doi.org/10.1021/jp100230c.
[89] Kumar P, Singh S, Hashmi SAR, Kim K-H. MXenes: emerging 2D materials for hydrogen storage. Nano Energy 2021;85:105989. https://doi.org/10.1016/j.nanoen.2021.105989.
[90] Hu Q, Sun D, Wu Q, Wang H, Wang L, Liu B, et al. MXene: a new family of promising hydrogen storage medium. J Phys Chem A 2013;117:14253–60. https://doi.org/10.1021/jp409585v.
[91] Chen G, Zhang Y, Cheng H, Zhu Y, Li L, Lin H. Effects of two-dimension MXene Ti3C2 on hydrogen storage performances of MgH2-LiAlH4 composite. Chem Phys 2019;522:178–87. https://doi.org/10.1016/j.chemphys.2019.03.001.
[92] Yadav A, Dashora A, Patel N, Miotello A, Press M, Kothari DC. Study of 2D MXene Cr2C material for hydrogen storage using density functional theory. Appl Surf Sci 2016;389:88–95. https://doi.org/10.1016/j.apsusc.2016.07.083.
[93] Li Y, Guo Y, Chen W, Jiao Z, Ma S. Reversible hydrogen storage behaviors of Ti2N MXenes predicted by first-principles calculations. J Mater Sci 2019;54:493–505. https://doi.org/10.1007/s10853-018-2854-7.
[94] Liu Y, Gao H, Zhu Y, Li S, Zhang J, Li L. Excellent catalytic activity of a two-dimensional Nb4C3Tx (MXene) on hydrogen storage of MgH2. Appl Surf Sci 2019;493:431–40. https://doi.org/10.1016/j.apsusc.2019.07.037.
[95] Jiang R, Xiao X, Zheng J, Chen M, Chen L. Remarkable hydrogen absorption/desorption behaviors and mechanism of sodium alanates in-situ doped with Ti-based 2D MXene. Mater Chem Phys 2020;242:122529. https://doi.org/10.1016/j.matchemphys.2019.122529.
[96] Fan Y, Chen D, Liu X, Fan G, Liu B. Improving the hydrogen storage performance of lithium borohydride by Ti3C2 MXene. Int J Hydrogen Energy 2019;44:29297–303. https://doi.org/10.1016/j.ijhydene.2019.01.011.
[97] Le TN-M, Chiu C, Kuo J-L. From the perspectives of DFT calculations, thermodynamic modeling, and kinetic Monte Carlo simulations: the interaction between hydrogen and Sc2C monolayers. Phys Chem Chem Phys 2020;22:4387–401. https://doi.org/10.1039/C9CP05796J.
[98] Li X, Ma X, Zhang J, Akiyama E, Wang Y, Song X. Review of hydrogen embrittlement in metals: hydrogen diffusion, hydrogen characterization, hydrogen embrittlement mechanism and prevention. Acta Metall Sin 2020;33:759–73. https://doi.org/10.1007/s40195-020-01039-7.
[99] Pradhan A, Vishwakarma M, Dwivedi SK. A review: the impact of hydrogen embrittlement on the fatigue strength of high strength steel. Mater Today Proc 2019;26:3015–9. https://doi.org/10.1016/j.matpr.2020.02.627.
[100] Dwivedi SK, Vishwakarma M. Hydrogen embrittlement in different materials: a review. Int J Hydrogen Energy 2018;43:21603–16. https://doi.org/10.1016/j.ijhydene.2018.09.201.
[101] Bhadeshia HKDH. Prevention of hydrogen embrittlement in steels. ISIJ Int 2016;56:24–36.

[102] Tamura Motonori. Hydrogen permeation characteristics of TiN-coated stainless steels. J Mater Sci Eng 2015;5:197–201. https://doi.org/10.17265/2161-6213/2015.5-6.002.
[103] Li X, Wang Y, Zhang P, Li B, Song X, Chen J. Effect of pre-strain on hydrogen embrittlement of high strength steels. Mater Sci Eng, A 2014;616:116–22. https://doi.org/10.1016/j.msea.2014.07.085.
[104] Barthélémy H. Effects of pressure and purity on the hydrogen embrittlement of steels. Int J Hydrogen Energy 2011;36:2750–8. https://doi.org/10.1016/j.ijhydene.2010.05.029.
[105] Song SW, Kim J-N, Seo HJ, Lee T, Lee CS. Effects of carbon content on the tensile and fatigue properties in hydrogen-charged Fe-17Mn-xC steels: the opposing trends. Mater Sci Eng, A 2018;724:469–76. https://doi.org/10.1016/j.msea.2018.03.117.
[106] Malitckii E, Yagodzinskyy Y, Vilaça P. Role of retained austenite in hydrogen trapping and hydrogen-assisted fatigue fracture of high-strength steels. Mater Sci Eng, A 2019;760:68–75. https://doi.org/10.1016/j.msea.2019.05.103.
[107] Gangloff RP. Hydrogen assisted cracking of high strength alloys. Alum Co Am Alcoa Cent Pa Alcoa Tech Cent; 2003.
[108] McMahon CJ. Hydrogen-induced intergranular fracture of steels. Eng Fract Mech 2001;68:773–88. https://doi.org/10.1016/S0013-7944(00)00124-7.
[109] Venezuela J, Liu Q, Zhang M, Zhou Q, Atrens A. The influence of hydrogen on the mechanical and fracture properties of some martensitic advanced high strength steels studied using the linearly increasing stress test. Corrosion Sci 2015;99:98–117. https://doi.org/10.1016/j.corsci.2015.06.038.
[110] Lynch SP. 2 - hydrogen embrittlement (HE) phenomena and mechanisms. In: Raja VS, Shoji T, editors. Stress corros. Crack. Woodhead Publishing; 2011. p. 90–130. https://doi.org/10.1533/9780857093769.1.90.
[111] Martin F, Leunis E, Briottet L, L P, Chêne J, M L. Comparison of the tensile behavior of a tempered 34CrMo4 steel exposed in situ to high pressure H2 gas or to cathodic H charging. SteelyHydrogen2014. Conf. Proc. 2014;2:448–61.
[112] Ramamurthy S, Atrens A. Stress corrosion cracking of high-strength steels. Corrosion Rev 2013;31:1–31. https://doi.org/10.1515/corrrev-2012-0018.
[113] Hooshmand Zaferani S, Miresmaeili R, Pourcharmi MK. Mechanistic models for environmentally-assisted cracking in sour service. Eng Fail Anal 2017;79:672–703. https://doi.org/10.1016/j.engfailanal.2017.05.005.
[114] Koyama M, Tasan CC, Akiyama E, Tsuzaki K, Raabe D. Hydrogen-assisted decohesion and localized plasticity in dual-phase steel. Acta Mater 2014;70:174–87. https://doi.org/10.1016/j.actamat.2014.01.048.
[115] Lynch SP. Progress towards understanding mechanisms of hydrogen embrittlement and stress corrosion cracking. Corrosion (Houston, TX, U S) 2007;2007:11–5. NACE-07493;01.
[116] Song J, Curtin WA. Atomic mechanism and prediction of hydrogen embrittlement in iron. Nat Mater 2013;12:145–51. https://doi.org/10.1038/nmat3479.
[117] Venezuela J, Liu Q, Zhang M, Zhou Q, Atrens A. A review of hydrogen embrittlement of martensitic advanced high-strength steels. Corrosion Rev 2016;34:153–86. https://doi.org/10.1515/corrrev-2016-0006.
[118] Lu G, Zhang Q, Kioussis N, Kaxiras E. Hydrogen-enhanced local plasticity in aluminum: an ab initio study. Phys Rev Lett 2001;87:95501. https://doi.org/10.1103/PhysRevLett.87.095501.
[119] Robertson IM. The effect of hydrogen on dislocation dynamics. Eng Fract Mech 1999;64:649–73. https://doi.org/10.1016/S0013-7944(99)00094-6.
[120] Liang Y, Ahn DC, Sofronis P, Dodds RH, Bammann D. Effect of hydrogen trapping on void growth and coalescence in metals and alloys. Mech Mater 2008;40:115–32. https://doi.org/10.1016/j.mechmat.2007.07.001.
[121] Venezuela J, Zhou Q, Liu Q, Li H, Zhang M, Dargusch MS, et al. The influence of microstructure on the hydrogen embrittlement susceptibility of martensitic advanced high strength steels. Mater Today Commun 2018;17:1–14. https://doi.org/10.1016/j.mtcomm.2018.07.011.
[122] Shen S, Song X, Li Q, Li X, Zhu R, Yang G. Effect of Cr x C y –NiCr coating on the hydrogen embrittlement of 17-4 PH stainless steel using the smooth bar tensile test. J Mater Sci 2019;54:7356–68. https://doi.org/10.1007/s10853-019-03356-4.
[123] Raabe D, Sun B, Kwiatkowski Da Silva A, Gault B, Yen HW, Sedighiani K, et al. Current challenges and opportunities in microstructure-related properties of advanced high-strength steels. Metall Mater Trans A Phys Metall Mater Sci 2020;51:5517–86. https://doi.org/10.1007/s11661-020-05947-2.
[124] Sun B, Wang D, Lu X, Wan D, Ponge D, Zhang X. Current challenges and opportunities toward understanding hydrogen embrittlement mechanisms in advanced high-strength steels: a review. Acta Metall Sin 2021;34:741–54. https://doi.org/10.1007/s40195-021-01233-1.
[125] Liu Q, Zhou Q, Venezuela J, Zhang M, Atrens A. The role of the microstructure on the influence of hydrogen on some advanced high-strength steels. Mater Sci Eng, A 2018;715:370–8. https://doi.org/10.1016/j.msea.2017.12.079.
[126] Li LX, Sun MH, Fan MC, Yang TS, Du FS. New Rapid prototyping technology for the prevention of hydrogen embrittlement of metal strips. Corrosion Sci 2020;164. https://doi.org/10.1016/j.corsci.2019.108341.
[127] Nemanič V. Hydrogen permeation barriers: basic requirements, materials selection, deposition methods, and quality evaluation. Nucl Mater Energy 2019;19:451–7. https://doi.org/10.1016/j.nme.2019.04.001.
[128] Stöver D, Buchkremer HP, Hecker R. Hydrogen and deuterium permeation through metallic and surface-oxidized chromium. Surf Coating Technol 1986;28:281–90. https://doi.org/10.1016/0257-8972(86)90085-X.
[129] Levchuk D, Levchuk S, Maier H, Bolt H, Suzuki A. Erbium oxide as a new promising tritium permeation barrier. J Nucl Mater 2007;367–370:1033–7. https://doi.org/10.1016/j.jnucmat.2007.03.183.
[130] Dwivedi SK, Vishwakarma M. Hydrogen embrittlement prevention in high strength steels by application of various surface coatings-A review. In: Singari RM, Mathiyazhagan K, Kumar H, editors. Lect. Notes mech. Eng. Singapore: Springer Singapore; 2021. p. 673–83. https://doi.org/10.1007/978-981-15-8542-5_58.
[131] Michler T, Naumann J. Coatings to reduce hydrogen environment embrittlement of 304 austenitic stainless steel. Surf Coating Technol 2009;203:1819–28. https://doi.org/10.1016/j.surfcoat.2009.01.013.
[132] Geim AK, Novoselov KS. The rise of graphene. Nat Mater 2007;6:183–91. https://doi.org/10.1038/nmat1849.
[133] Zou C, Yang B, Bin D, Wang J, Li S, Yang P, et al. Electrochemical synthesis of gold nanoparticles decorated flower-like graphene for high sensitivity detection of nitrite. J Colloid Interface Sci 2017;488:135–41. https://doi.org/10.1016/j.jcis.2016.10.088.
[134] Zhang K, Xiong Z, Li S, Yan B, Wang J, Du Y. Cu3P/RGO promoted Pd catalysts for alcohol electro-oxidation. J Alloys Compd 2017;706:89–96. https://doi.org/10.1016/j.jallcom.2017.02.179.
[135] Bunch JS, Verbridge SS, Alden JS, van der Zande AM, Parpia JM, Craighead HG, et al. Impermeable atomic

membranes from graphene sheets. Nano Lett 2008;8:2458–62. https://doi.org/10.1021/nl801457b.
[136] Kim Y-S, Kim J-G. Electroplating of reduced-graphene oxide on austenitic stainless steel to prevent hydrogen embrittlement. Int J Hydrogen Energy 2017;42:27428–37. https://doi.org/10.1016/j.ijhydene.2017.09.033.
[137] Brandolt C de S, Noronha LC, Hidalgo GEN, Takimi AS, Schroeder RM, Malfatti C de F. Niobium coating applied by HVOF as protection against hydrogen embrittlement of API 5CT P110 steel. Surf Coating Technol 2017;322:10–8. https://doi.org/10.1016/j.surfcoat.2017.05.017.
[138] Li X, Chen L, Liu H, Shi C, Wang D, Mi Z, et al. Prevention of hydrogen damage using MoS2 coating on iron surface. Nanomaterials 2019;9. https://doi.org/10.3390/nano9030382.
[139] Zhou P, Li W, Li Y, Jin X. The effect of MoS 2 content on the protective performance of Ni-MoS 2 composite coatings against hydrogen embrittlement in high strength steel. J Electrochem Soc 2017;164:D23–9. https://doi.org/10.1149/2.0421702jes.
[140] Zhou P, Li W, Jin X. Comparison of hydrogen permeation properties of pure Ni, Ni-MoS 2 , Ni-graphene composite coatings deposited on quenching and partitioning steel and the hot-dipping galvanized steel. J Electrochem Soc 2017;164:D394–400. https://doi.org/10.1149/2.0501707jes.
[141] Seel M, Pandey R. Proton and hydrogen transport through two-dimensional monolayers. 2D Mater 2016;3:25004. https://doi.org/10.1088/2053-1583/3/2/025004.
[142] Kumar JA, Prakash P, Krithiga T, Amarnath DJ, Premkumar J, Rajamohan N, et al. Methods of synthesis, characteristics, and environmental applications of MXene: a comprehensive review. Chemosphere 2022;286:131607. https://doi.org/10.1016/j.chemosphere.2021.131607.
[143] Naguib M, Kurtoglu M, Presser V, Lu J, Niu J, Heon M, et al. Two-dimensional nanocrystals produced by exfoliation of Ti3AlC2. Adv Mater 2011;23:4248–53. https://doi.org/10.1002/adma.201102306.
[144] Montazeri K, Currie M, Verger L, Dianat P, Barsoum MW, Nabet B. Beyond gold: spin-coated Ti3C2-based MXene photodetectors. Adv Mater 2019;31:1903271. https://doi.org/10.1002/adma.201903271.
[145] Ding L, Wei Y, Li L, Zhang T, Wang H, Xue J, et al. MXene molecular sieving membranes for highly efficient gas separation. Nat Commun 2018;9:155. https://doi.org/10.1038/s41467-017-02529-6.
[146] Shen J, Liu G, Ji Y, Liu Q, Cheng L, Guan K, et al. 2D MXene nanofilms with tunable gas transport channels. Adv Funct Mater 2018;28:1801511. https://doi.org/10.1002/adfm.201801511.
[147] Fan Y, Li J, Wang S, Meng X, Zhang W, Jin Y, et al. Voltage-enhanced ion sieving and rejection of Pb2+ through a thermally cross-linked two-dimensional MXene membrane. Chem Eng J 2020;401:126073. https://doi.org/10.1016/j.cej.2020.126073.
[148] Ren D, Liu Y, Huang N. Chemical bonding states of TiC films before and after hydrogen ion irradiation. J Wuhan Univ Technol Sci Ed 2007;22:630–3. https://doi.org/10.1007/s11595-006-4630-9.
[149] Shi K, Meng X, Xiao S, Chen G, Wu H, Zhou C, et al. Mxene coatings: novel hydrogen permeation barriers for pipe steels. Nanomaterials 2021;11. https://doi.org/10.3390/nano11102737.
[150] Tamura M. Hydrogen permeation of multi-layered-coatings. Adv Mater Res 2019;1152:9–18. https://doi.org/10.4028/www.scientific.net/amr.1152.9.